Antimicrobial Activity of Gold-Titanates on Gram-positive Cariogenic Bacteria

Trinuch Eiampongpaiboon

A dissertation

submitted in partial fulfillment of the

requirements for the degree of

Doctor of Philosophy

University of Washington

2014

Reading Committee:

Daniel C.N. Chan, Chair

Whasun O. Chung, Co-Chair

James D. Bryers

Program Authorized to Offer Degree:
Oral Biology

University of Washington

Abstract

Antimicrobial Activity of Gold-Titanates on Gram-positive Cariogenic Bacteria

Trinuch Eiampongpaiboon

Chair of the Supervisory Committee:
Professor Daniel C.N. Chan
Department of Restorative Dentistry
Research Professor Whasun O. Chung
Department of Oral Health Sciences

Gram-positive cariogenic bacteria are important etiological agents in dental caries; therefore, strategies to inhibit these bacteria to reduce the incident of this disease have intensified. Antimicrobial activity of gold-titanates against several bacteria has recently been explored. Monosodium titanate (MST), nanomonosodium titanate (nMST), and amorphous peroxo-titanate (APT) are inorganic compounds with high binding affinity for specific metal ions or compounds such as gold (Au), palladium (Pd), and platinum (Pt). Titanates have been used as an ion exchanger binding to the metal ions and act as a carrier. In this study, we investigated antibacterial activities of titanates and gold-titanates against *Actinomyces viscosus*, *Lactobacillus casei*, and *Streptococcus mutans,* which are important Gram-positive cariogenic bacteria as well as *Streptococcus gordonii*, non-pathogenic oral bacteria. Total bacterial proteins were extracted and measured to represent total bacterial cell mass after 24 h incubation. We found all gold-titanates and APT alone significantly reduced bacterial protein content for *L. casei* and *A. viscosus* while only MST-Au(III) and nMST-Au(III) affected *S. mutans*. Total cell mass of *S.*

gordonii was significantly decreased when exposed to gold-titanates vs. to titanates alone. Overall, nMST-Au(III) showed the most effectiveness against all bacteria at 400 mg/L. We further examined the effect of gold-titanate nanoparticles (NPs) nMST-Au(III) concentration (10,200,400 mg/L) on *L. casei* and *S. mutans* cell viability over time via Live/Dead (L/D) direct cell fluorescent staining and colony forming units (CFUs). The L/D staining showed all three concentrations of nMST-Au(III) affected *L. casei* growth but only 200 and 400 mg/L nMST-Au(III) interrupted *S. mutans* growth. The growth curves based on CFUs/mL showed all nMST-Au(III) concentrations affected growth of both *L. casei* and *S. mutans.* Transmission electron microscopy (TEM) was used to determine specific locations on all four bacteria (*A. viscosus*, *L. casei, S. gordonii* and *S. mutans*) affected by the nMST-Au(III). TEM images showed gold-titanate NPs attached to the bacterial cell wall and were internalized into all bacteria. Small-scale transcriptomics relating to *S. mutans* selected metabolic functions were monitored to quantify the mechanism of antibacterial activity of gold-titanate NPs, using quantitative reverse transcription-polymerase chain reaction (QRT-PCR). We found the mRNA expression of *S. mutans* genes responded to nMST-Au(III) in different manner when exposed to various concentrations and times. Genes related to bacterial stress response were up-regulated when exposed to medium and high concentrations at both 6 and 10 h. These suggest that gold-titanate NPs cause environmental stress to *S. mutans*. Gold-titanate NPs demonstrated potential antimicrobial activity against Gram-positive cariogenic bacteria. These results support further development of gold-titanate NPs as a potential novel material to prevent dental caries.

DEDICATION

To the Kingdom of Thailand,

My Parents, Family, and all Mentors

ACKNOWLEDGMENTS

First and foremost, I would like to express my deep gratitude to my advisors, Dr. Daniel Chan and Dr. Whasun Chung, Chairs of my thesis supervisory committee for their continued support, guidance, and encouragement. Also, I cannot express enough thanks to my supervisory committee, Dr. James Bryers, Dr. Kwok-Hung (Albert) Chung, Dr. John Wataha, and Dr. Natasha Flake, for their invaluable suggestion and guiding on my research for this past several years.

I wish to express my sincere thanks to Dr. Martha Somerman for her kind support and guidance. I would also like to thank members of Dr. Somerman's lab especially Dr. Brian Foster who was teaching me research techniques during the first two years of my PhD study.

I take this opportunity to thank Dr. Hanson Fong and Edward Parker for helping me in electron microscopy experiment, and Dr. Charles Spiekerman for providing statistical consultation. My research would not have been possible without their helps.

Many thanks to Dennis DiJulio, Sucheol Gil, Jeanie Drury, and other members of Dr. Chung's lab for their encouragement, support, and friendship. Also, special thanks go to Dan Fisher, Dr. Karen Smith, and members of Dr. Bryers' lab for their great help and support.

My completion of this project could not have been accomplished without the support from faculties, staffs and my classmates in Oral Biology program.

On top of that, I am in debt to faculties and staffs in Department of Prosthodontics, Faculty of Dentistry, Mahidol University for allowing me to take study leave.

I would like to express my deep gratitude to Ministry of Science and Technology, Thailand, for financial support and NIH for project funding throughout my doctoral degree study.

Without questions, I deeply thank to my parents, sisters, brothers, nieces, and nephews for their unconditional love, support, and encouragement.

TABLE OF CONTENTS

LIST OF FIGURES

LIST OF TABLES

CHAPTER 1

INTRODUCTION

CARIOGENESIS

Dental caries is a common oral disease, which can be found in both children and adult but it can progress to severe inflammation of dental pulp and/or periapical tissues leading to tooth loss. The prevention of this disease helps improve oral health care and reduces treatment cost. The caries process consists of both remineralization and demineralization. There are many factors that can shift the balance of these processes. Sugar and bacteria are the dominant factors shifting the balance toward net mineral loss, which leads to initiation and progression of dental caries (Hara and Zero, 2010). *Streptococcus mutans*, facultative anaerobic Gram-positive bacteria, are the major pathogens of human dental caries and are frequently isolated from cavitated caries lesions and possess high acidogenicity and aciduricity. Also, *S. mutans* can produce surface antigens I/II and water-insoluble glucans that promote bacterial adhesion to the tooth surface and to other bacteria, leading to biofilm formation (Tanzer *et al.*, 2001; Matsui and Cvitkovitch, 2010; Takahashi and Nyvad, 2010). *Lactobacillus casei,* facultative anaerobic Gram-positive bacteria, have been detected in dental biofilms covering white-spot lesions and have also been determined to be cariogenic bacteria because of their capacity to produce acids as well as their ability to grow and survive in an acidic environment (Badet and Thebaud, 2008). Non-mutans acidogenic and aciduric bacteria, including non-mutans Streptococci and *Actinomyces viscosus* are more closely involved with the initiation of dental caries. They are regarded as early colonizers of tooth surfaces, whereas *S. mutans* are considered to be late

colonizers (Sansone *et al*., 1993; Takahashi and Nyvad, 2008; Ramalingam *et al*., 2012).

NANOPARTICLES (NPS) AND THEIR ANTIMICROBIAL ACTIVITIES

Many recent studies have revealed that nanoparticles (NPs) have various properties that can be exploited in many biomedical applications. Silver, gold, platinum, palladium, and zinc oxide have been used as antimicrobial agents (Amarnath *et al*., 2012; Jayaseelan *et al*., 2012; Lopes *et al*., 2012; Ma *et al*., 2012; Mohanty *et al*., 2012). NPs are able to act as a carrier of drugs or to concentrate drugs on their surfaces, which results in polyvalent effects that enhance drug efficacy (Thomas and Klibanov, 2003; Rosi *et al*., 2006; Cho *et al*., 2010). Also NPs themselves can specifically attack biological targets after modification with targeting molecules (Bowman *et al*., 2008; Gutierrez *et al*., 2009).

A recent study reported that silver nanoparticles (AgNPs) could deliver Ag+ ion to bacteria via attacking bacterial cytoplasm and cell membrane (Xiu *et al*., 2012). In addition, Su *et al*. (2009) found that physical contact of AgNPs and bacterial cell wall initiated bacterial cell death. AgNPs may cause a loss of membrane integrity, increase the production of intracellular reactive oxygen species (ROS), and inactivate the energy-dependent mechanism. AgNPs have developed as a new antimicrobial agent due to their high surface area to volume ratio, chemical, and physical properties (Rai *et al*., 2010). Several forms of silver such as silver zeolite, silver sulfadiazine, or metallic silver can be used as antibacterial agents. However, silver toxicity has been reported in previous studies, such as cytotoxicity of AgNPs to mitochondria activity, fibroblast and keratinocyte cultures, and rat liver cell lines (Hussain *et al.,* 2005; Burd *et al*., 2007).

Gold nanoparticles (AuNPs) were discovered in 1857. They have been recommended for

different purposes such as labeling and imaging, clinical diagnostics, and therapeutics (Boisselier *et al*., 2009; Wang *et al*., 2012; Zhou *et al*., 2012; MubarakAli *et al*., 2013). Antimicrobial activity of AuNPs has been studied with several microorganisms. Zhao *et al*. (2010) synthesized AuNPs with positively charged molecules as ligands to increase permeability of the bacterial cell wall. They proposed amino-substituted pyrimidine-capped AuNPs to target *Pseudomonas aeruginosa* and *E. coli*, which are Gram-negative bacteria. These pyrimidine-capped AuNPs were able to disrupt the bacterial cell membranes leading to leakage of cytoplasmic components, including nucleic acid. NPs also internalized into bacterial cells, resulting in interaction with deoxyribonucleic acid (DNA) and inhibition of protein synthesis. Wang *et al*. (2011) studied the toxic effects of AuNPs on *Salmonella typhimurium* and found that transmission electron microscopy (TEM) images illustrated AuNPs were adsorbed onto bacterial cell walls but could not be internalized into bacterial cells. According to Zhou *et al*. (2012), *E. coli* exposed to AuNPs were reduced in bacterial cell number during their exponential phase. They found that not only shape and size of AuNPs but also surface modification plays an important role in antibacterial activity.

Molecular mechanisms of action of AuNPs on several types of bacteria have been investigated. Cui *et al*. (2012) found that AuNPs exerted their antibacterial activities on *E.coli* mainly in two ways. One was to collapse membrane potential and induce the down-regulation of oxidative phosphorylation pathway {F-type Adenosine triphosphate (ATP) synthase and ATP level}, indicating a general decline in metabolism. Another mechanism was to inhibit tRNA function, indicating a collapse of biological process. Also, positive charges on metal-ions would relate to their antibacterial activity, since this characteristic allows for the electrostatic attraction between the negative charges of bacterial cell wall/membrane and positive charges of

nanoparticles. Silvestry-Rodriguez *et al*. (2008) suggested that anionic polysaccharides of Gram-negative bacteria were significant molecules for NPs biosorption.

Hajipour *et al.* (2012) reported possible toxicity mechanisms of various NPs against bacteria. They suggest that NPs are able to

- Attach to bacterial membranes by electrostatic interaction and disrupt membrane integrity.
- Induce oxidative stress by free radical formation such as reactive oxygen species (ROS) and hydroxyl radical and damage essential proteins and DNA.
- Have "weak mutagenic potential" that would induce frame shift mutation in *S. typhimurium*.
- Increase peroxidation of the polyunsaturated phospholipid component of the lipid membrane and promote the disruption of "cell respiration".
- Not only be internalized into bacterial cells but also locally change microenvironment and increase NPs solubility, which cause bacterial damage.
- Bind to DNA and inhibit DNA unwinding causing bacterial cell death.
- Bind to sulfur, oxygen, and nitrogen of essential biological molecules leading to inhibiting bacterial growth.

Correspondingly, Ul-Islam *et al.* (2014) reviewed the possible antibacterial mechanism of NPs. Three particular mechanisms of NPs were (1) interaction to bacterial cell membrane, (2) generation of ROS, and (3) uptake of free metallic ions, which leads to damaging bacterial structure, interrupting bacterial normal metabolic functions, and causing bacterial cell death.

ORAL APPLICATIONS OF ANTIMICROBIAL AGENTS

Microbial infection is the main factor relating to dental caries and periodontal disease. Therefore, antimicrobial agents have been widely used in dentistry to prevent or reduce incident of these diseases. Antimicrobial polymers, peptides, NPs, or antibiotics have been developed to prevent and/or reduce bacterial growth and adhesion (Imazato, 2009; García-Contreras *et al*., 2011; Liu *et al*., 2011; He *et al*., 2014). These antimicrobial agents have been used in different applications. For example, He *et al*. (2014) introduced a novel-antibiotic-decorated titanium as a potential dental implant material. This material was tested for efficacy against *S. mutans* and *E. coli* bacterial adhesion and proliferation. The authors found that incorporating cefotaxime sodium onto titanium implant surface enhanced prevention of *E. coli* and *S. mutans* adhesion and proliferation. However, antibiotic drug-resistant has been an important issue to consider in the use antibiotic. Several studies report both pathogenic and non-pathogenic Gram-positive oral bacteria were able to develop antibiotic resistance. Both resistance to antibiotic drugs (e.g. penicillin, tetracycline, cephalosporin, erythromycin and metronidazole) and resistance to other antimicrobial agents such as chlorhexidine were observed in the oral flora (Roberts, 1998; Sweeney *et al*., 2004). Roberts and Mullany (2010) gave a comprehensive review that biofilm structural properties enhanced antibiotic resistance gene transfer among the close proximity of bacterial cells within the biofilm, and the biofilm matrix is a main reservoir of these antibiotic resistance genes for bacteria in the oral cavity.

Antimicrobial peptides have been studied to control oral pathogenic bacteria. Liu *et al*. (2011) studied the effect of decapeptide KSL (KKVVFKVKFK-NH_2) on oral pathogens, including periodontal pathogens (e.g. *Porphyromonas gingivalis*, *Aggregatibacter actinomycetemcomitans*, and *Fusobacterium nucleatum*), cariogenic bacteria (e.g. *S. mutans*, *A.*

viscosus, and *Lactobacillus acidophilus*) and the yeast, *Candida albicans*. They found that *S. mutans* and *L. acidophilus* were the most susceptible organisms to KSL. KSL also affected *S. mutans* biofilm formation. They suggested that this peptide might have a potential to kill *S. mutans* in dental plaque. However, Rocha da Silva *et al*. (2012) suggested that antimicrobial peptides have some limitations for therapeutic use in that their high cationic activity may be reduced in biological fluids including saliva.

Oral applications of nanoparticles have recently been considered (Allaker, 2010). The potential of NPs to control oral biofilm formation is related with their biocidal and anti-adhesive capabilities. NPs have been incorporated into dental materials to improve antimicrobial activity. Silver, gold, copper, titanium, and zinc are potential NPs for the use in dental field, which are similar to their use in medical areas. Also, nanoparticulate metal oxides have been selected since their unusual crystal morphologies increase the number of edges and corners of NPs, which generates high surface of NPs to interact with bacteria. Antifungal and antiviral actions have also been investigated. Nevertheless, the concern of NPs biocompatibility has been questioned. Therefore, understanding mechanism of NPs action would be an important issue before clinical application.

TITANATES AND GOLD-TITANATES

Monosodium titanate (MST) and amorphous peroxotitanate (APT) are inorganic ion-exchangers that can bind with several metal ions such as gold, palladium, and platinum. These materials were modified and produced by the group from Savannah River National Laboratory (Hobbs *et al*., 2005; Hobbs, 2011). In previous studies, MST and APT were used as sorbents/ion exchangers for removal of radionuclides from nuclear wastes (Hobbs *et al*., 2005; Nyman and

Hobbs, 2006). As mentioned before, sodium titanates and peroxotitanate have been studied for their capacity to exchange titanates to deliver therapeutic ions to target cells or to inhibit the bacterial growth (Davis *et al*., 2009; Wataha *et al*., 2009; Wataha *et al*., 2010; Chung *et al*., 2011). Antibacterial effect of titanates without metal ions was also observed and it was found that they did not inhibit bacterial growth (Chung *et al*., 2011). Metal-ions would play the role as antimicrobial agents, whereas titanates themselves could work as stabilizers and release the ions to target cells.

Davis *et al.* (2007) studied *in vitro* biological effects of monosodium titanates and amorphous peroxo-titanates on mammalian cells. They found MST at concentrations of 100 mg/L caused a 25% reduction in succinate dehydrogenase (SDH) activity, an indication of cell mitochondrial activity in monocytes and fibroblasts. APT showed minor changes in SDH activity in both monocytes and fibroblasts (<15%) but no significant change of TNF-alpha secretion from monocytes was detected. The authors claimed that only slight cytotoxicity of MST and APT was observed *in vitro*, and both of them are considered to use in biological environments. Drury *et al*. (2014) studied biological effects of MST and nano-sized MST (nMST) with and without metals on two human cell lines, gingival carcinoma cells (OSC2) and lung fibroblasts (WI-38). Their results showed that MST at concentrations higher than 50 mg/L significantly decreased mitochondrial activity of both cell types by 50% over untreated cultures. Nano-sized MST significantly suppressed mitochondrial activity in a rapidly dividing cell line, OSC2 cells whereas nMST had minimal inhibitory effects on WI-38 cell line, even at concentration ≤ 200 mg/L. However, the mechanism of titanates or metal-titanates antimicrobial activity is currently not completely understood.

STREPTOCOCCUS MUTANS GENE FUNCTIONS RESPONDING TO EXTERNAL STIMULI

In 2002*, S. mutans* UA159 genome, a serotype c strain, was completely sequenced by Ajdić *et al*. It is composed of 2,030,936 base pairs and contains 1,963 open reading frames (ORFs), 63% of which have been assigned putative functions. Owing to this complete genome sequences, we are able to further study *S. mutans* response to external stimuli. Genes relating to several biological functions such as cell wall synthesis, specific metabolic pathways, ion transport, and specific virulence factors are present in *S. mutans* genomic sequences.

External stimuli from dynamic condition changes in the oral cavity place multiple stresses on oral bacteria and can induce stress-response proteins. Previous studies have reported several mechanisms involved in the survival of *S. mutans* under stress conditions. Proton pumps, membrane composition changes, alteration of metabolic pathways and protection and/or repair of macromolecules are common mechanisms of acid tolerance for Gram-positive bacteria (Hasona *et al*., 2006; Li *et al*., 2014). Bowden and Hamilton (1998) suggested that oral bacteria would respond to each stress factor in a different manner. For example, with low pH condition, oral bacteria would increase glycolytic and ATPase activity, as well as enhance expression of key acid-responsive genes. With increased oxygen concentrations, supragingival plaque microflora would stimulate hydrogen peroxide production and induction of Nicotinamide Adenine Dinucleotide (NADH) oxidase.

Two signal-transducing two-component systems (TCS) play a key role in bacterial adaptation, survival, and stress tolerance of *S. mutans* by sensing changes in environment and modulating gene expression in response to external stimuli (Li *et al*., 2002; Ahn *et al*., 2006). TCS consists of a membrane-associated histidine kinase sensor (*CiaH*), a sensor protein that

perceives environmental change, and a cytoplasmic response regulator that enables cellular response via regulation of gene expressions when stimulated. High temperature requirement A (*HtrA*), a family of serine protease, is regulated by the two-component regulatory system that senses and responds to periplasmic stress such as protein misfolding and aggregation. In *S. mutans*, *HtrA* is important for the biogenesis of extracellular proteins, including surface-associated glycolytic enzyme and thus for biofilm formation. *HtrA* works as a multifunctional chaperone and protease to contribute in part of protein quality control. *HtrA* also performs to be a part of regulatory network that coordinates cellular growth, stress tolerance, and biofilm formation (Biswas S and Biswas I, 2005; Kang *et al*., 2010)

BrpA (biofilm regulatory protein A) is involved in acid and oxidative stress tolerance responses and biofilm development by *S. mutans* (Wen *et al*., 2006; Bitoun et al., 2012). Wen *et al.* (2006) found that *BrpA* deficiency has no significant impact on *S. mutans* growth rate in planktonic culture but bacteria were likely to form chains more than wild type. Also, decreasing *BrpA* leads to increasing bacterial autolysis. The author suggested that *BrpA* functions relate mostly to cell accumulation/biofilm development but not to initial adherence.

RESEARCH GOALS AND SPECIFIC AIMS

Gram-positive cariogenic bacteria are important etiological factors of dental caries, which are significant oral health problem. A previous study by Chung *et al*. (2011) studied the effect of metal-titanate compounds and titanates alone on Gram-negative periodontal pathogens such as *A. actinomycetemcomitans*, *P. gingivalis,* and *Prevotella intermedia.* They found particles of MST with gold were highly effective in inhibiting bacterial growth. Similarly, other studies found gold NPs themselves have antimicrobial activity against Gram-negative bacteria (Zhao *et al*., 2010; Cui *et al*., 2012; Lopes *et al*., 2012). Conversely, antimicrobial properties of metal-titanate particles against Gram-positive cariogenic bacteria are still unknown. Recently, nano-sized sodium titanate particles have been developed; reducing particle size, increasing surface area, but maintaining similar morphology as well as chemical composition compared to micron-sized sodium titanates (Elvington *et al*., 2012). Previous studies have shown interactions between gold nanoparticles and bacteria, including biosorption, NPs breakdown or aggregation, and cellular uptake vary depending on size, shape, and surface functional group of gold nanostructures. (Cho *et al*., 2010; Lopes *et al*., 2012). A mechanistic study of metal nanoparticles-bacterial interaction would assess the potential of using these biomaterials as antibacterial agents. Currently, studies on oral bacterial gene expression responding to metal NPs have been incomplete. Understanding genes relating to bacterial stress responses, ATP-binding cassette (ABC) transporters, biofilm formation, glucans production, and cell wall synthesis would help determine whether or not antibacterial activity of NPs affects oral bacterial functions.

Our experiments would provide answers to whether gold-titanates could be used as antibacterial agents against Gram-positive cariogenic bacteria that are significant causes of dental caries. Investigating their mechanism of action on bacteria would give us better

understanding of their effects before their potential use in the oral cavity. Regarding clinical applications, we would apply these agents in dental materials; incorporating gold-titanates into restorative materials or devices could improve their antimicrobial properties to potentially reduce caries initiation and also secondary caries risk.

The overall hypothesis of our study is that nano-sized gold-titanates have an antimicrobial activity against Gram-positive cariogenic bacteria by affecting bacterial morphology and metabolic functions. To verify this hypothesis, we are proposing three specific aims.

Specific Aim 1: **To determine the antimicrobial effect of micro- and nano-sized titanates and gold-titanates on three cariogenic bacteria and non-pathogenic bacteria.**

In a previous study (Chung *et al.*, 2011), the concentration of micro-sized metal-titanates was limited at 25mg/L because their colloidal characteristic interfered with the optical density (OD) method of determining cell numbers. Our initial goal was to develop a method to examine antibacterial activity of gold-titanates with the concentration higher than 25mg/L. Here, the decision was to use bacterial protein level to represent total bacteria cell mass.

This aim was to compare antibacterial activity of micro-sized (MST and APT) and nano-sized (nMST) titanates, with and without gold particles in different concentrations on three Gram-positive cariogenic bacteria (*S. mutans*, *L. casei, and A. viscosus*) and control non-pathogenic bacteria (*Streptococcus gordonii*). Antimicrobial activity of the different concentrations of titanates and gold-titanates was determined by comparing the bacterial cell mass based on protein counted between control and treated groups. Bacterial proteins were extracted and the bicinchoninic acid (BCA) protein assay was used to determine bacterial protein

levels that would represent total bacterial cell mass.

Specific Aim 2: **To determine bacterial growth rate and effect of the nMST-Au(III) in different time points.**

Total protein concentration represents only bacterial cell mass but this parameter could not distinguish live from dead bacteria or if the bacterial growth rate was inhibited. Live and dead fluorescent staining would provide the number of viable and dead cells when they were exposed to nMST-Au(III). Time-lapse measurements would quantify gold-titanate NPs effects on bacterial growth.

Live and dead analysis was used to determine the normal bacterial batch growth curve and the effect of nMST-Au(III) on bacterial growth over time. We quantified the action of titanates on bacterial growth curve until the stationary phase of growth. Colony forming units (CFU) were also used to quantify the total viable bacterial cells.

Specific Aim 3: To determine the mechanism of gold-titanates action on bacteria by using sub-microscopic observation and quantitative gene expression responses.

Our goal in this aim is to investigate bacterial morphology and gene expression after exposure to nMST-Au(III) to define possible bacterial responses to these materials. Transmission electron microscopy (TEM) was used to determine which specific areas on or in Gram-positive bacterial cells were affected by gold-titanates. In addition, changes of *S. mutans* messenger ribonucleic acid (mRNA) expression of various key genes after treatment with various concentrations of nMST-Au(III) were determined by quantitative reverse transcription-polymerase chain reaction (QRT-PCR). Genes related to bacterial stress responses, ABC

transporters, biofilm formation, glucans production, and cell wall synthesis were monitored to investigate whether antibacterial activity of gold-titanates affected these bacterial functions.

CHAPTER 2

BACTERIA&TITANATES

BACTERIAL STRAINS AND GROWTH CONDITIONS

For this study, the bacteria we studied are part of an established oral microbial consortium (Table 2.1).

Actinomyces viscosus (ATCC® 43146) was cultured under anaerobic condition in Trypticase Soy broth (BD#211825, Difco Laboratories) supplemented with yeast (1g/L), 0.5 mg/mL/L hemin, and 5mg/mL/L vitamin K.

Lactobacillus casei (ATCC® 15008) was cultured aerobically at 37°C in 55 g/L Difco™ Lactobacilli MRS broth (BD#2388130, Difco Laboratories, Becton Dickinson, Franklin Lakes, NJ).

Streptococcus mutans UA 159 (ATCC® 700610) and *Streptococcus gordonii* (ATCC® 49818) were cultured aerobically at 37°C in 37 g/L Bacto™ Brain Heart Infusion (BHI) broth (BD#237500, Difco Laboratories).

All bacteria were cultivated in suspended batch culture from frozen stocks; the absence of contamination was verified at each thaw via Gram stain and periodically with bacteria-specific primer and quantitative polymerase chain reaction. All bacteria were grown overnight before inoculation into experimental cultures.

COLONY FORMING UNITS/OPTICAL DENSITY

: Calculating the Number of Bacteria per mL of Serially Diluted Bacteria:

To calculate the number of bacteria per mL of diluted sample, the following equation is used:

$$\frac{\text{Number of CFU}}{\text{Volume plated (mL) x total dilution used}} \longrightarrow \frac{\text{Number of CFU}}{\text{mL}}$$

A spectrophotometer was used to measure the optical density (OD) of bacterial sample at 595 nm. Knowing the CFU and optical density, we calculated colony forming unit per optical density (CFU/A) for each bacterial species (Table2.2).

DETERMINING PARTICLE SIZE AND FLUORESCENCE OF nMST-Au(III)

Dynamic light scatter (DLS, Malvern®) is used to determine the size distribution profile of small particles in suspension. nMST-Au(III) at concentration of 10 mg/L was used to determine the particle size. The average size of nMST-Au(III) at 10 mg/L is 420.3 ± 32.31 nm (Figure 2.1). Transmission electron microscopy (TEM) images showed gold particles bound within nMST (Figure 2.2). Additionally, when we observed nMST-Au(III) under UV light, nMST-Au(III) did fluorescence (Figure 2.3).

PREPARATION OF TITANATES

Micro-sized and nano-sized of monosodium titanate (MST and nMST), and amorphous peroxotitanate (APT) were prepared using a sol-gel or hydrothermal synthetic techniques as described in previous studies (Hobbs *et al*., 2005; Hobbs, 2011; Elvington *et al*., 2012). $HAuCl_4 \bullet 3H_2O$ was combined with a suspension of MST, nMST, or APT for Au ion exchanger experiment to get MST-Au(III), nMST-Au(III), and APT-Au(III). Titanate and gold-titanate materials were prepared and sent to University of Washington from Dr. David Hobbs group

(Savannah River National Laboratory, Alken, SC). After that, titanates and gold titanates solution were prepared in sterile water. Each titanate was kept in 15 ml polyethylene tube covered by aluminum foil to avoid light exposure. The final concentration of stock titanates and gold-titanates were 4000, 2000, 1000, 500, 250, and 100 mg/L.

Bacteria	Bio-Safety Level	ATCC	Gram-Stain/ morphology/size	Growth condition
Actinomyces viscosus	BSL 2	43146	Positive/ thin branching bacillus/ 0.5x1.7-2.9 µm	Anaerobic, 37°C, 80%N2-10%CO2-10% H.
Lactobacillus casei; Strain L 944	BSL 1	15008; strain L 944	Positive/ rod shape growing in chain or pair/ 0.7-1.1 x 2.0- 4.0 µm	Facultative Anaerobe, 37°C Cultured in aerobic condition
Streptococcus gordonii	BSL 2	49818	Positive/ cocci grow in chains or pairs/ diameter of each cell ≈ 0.5 µm	Facultative Anaerobe, 37°C; Cultured in aerobic condition.
Streptococcus mutans UA 159	BSL 1	700610	Positive/ cocci grow in chains or pairs / diameter of each cell ≈ 0.5 µm	Facultative Anaerobe, 37°C; Cultured in aerobic condition.

Table 2.1: Oral microbes used in this study

Bacteria	*CFU/OD$_{595}$*
Streptococcus mutans	8.17E+07 cells/ A°
Streptococcus gordonii	1.93E+08 cells/ A°
Lactobacillus casei	2.60E+08 cells/ A°
Actinomyces viscosus	6.50E+07 cells/ A°

Table 2.2: Bacterial CFU vs OD$_{595}$

		Size (r.nm):	% Intensity	Width (r.nm):
Z-Average (r.nm): 344.1	Peak 1:	210.1	100.0	44.18
PdI: 0.524	Peak 2:	0.000	0.0	0.000
Intercept: 0.974	Peak 3:	0.000	0.0	0.000

Result quality : Refer to quality report

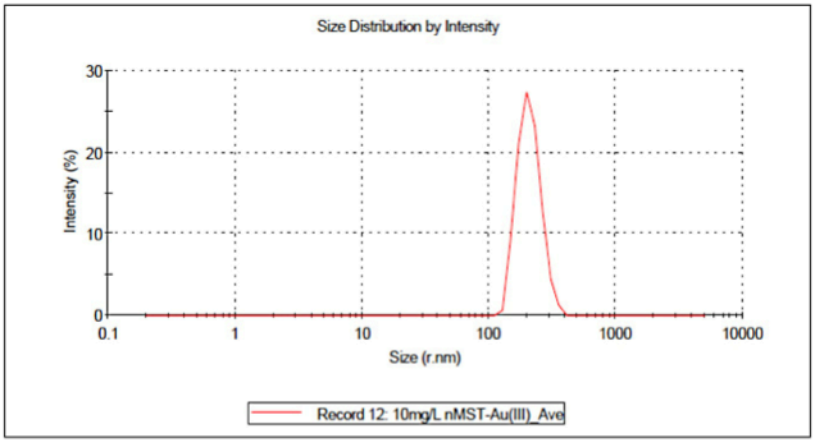

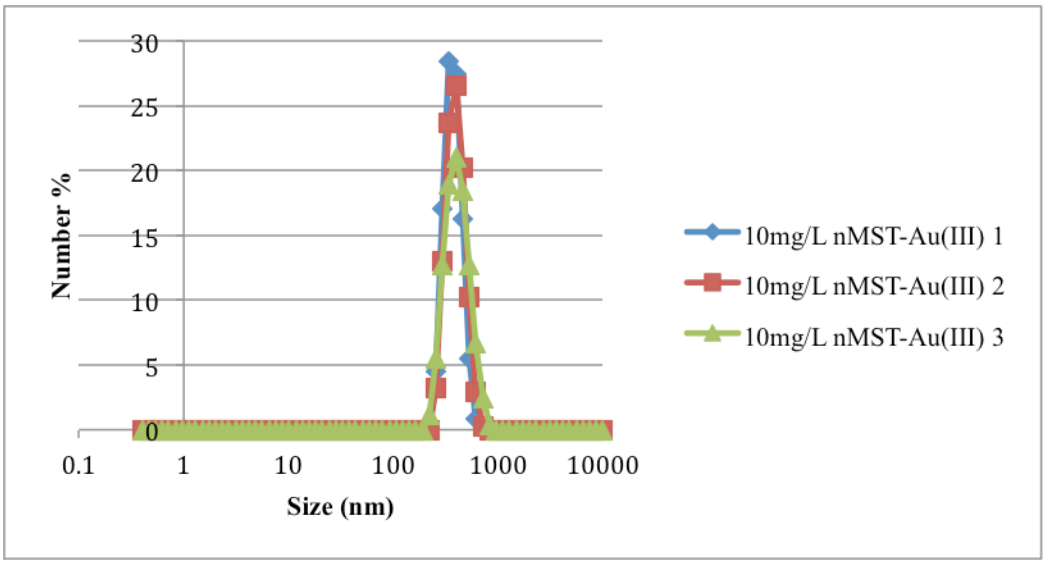

Figure 2.1: The average size of nMST-Au(III) is 420.3 ± 32.31 nm

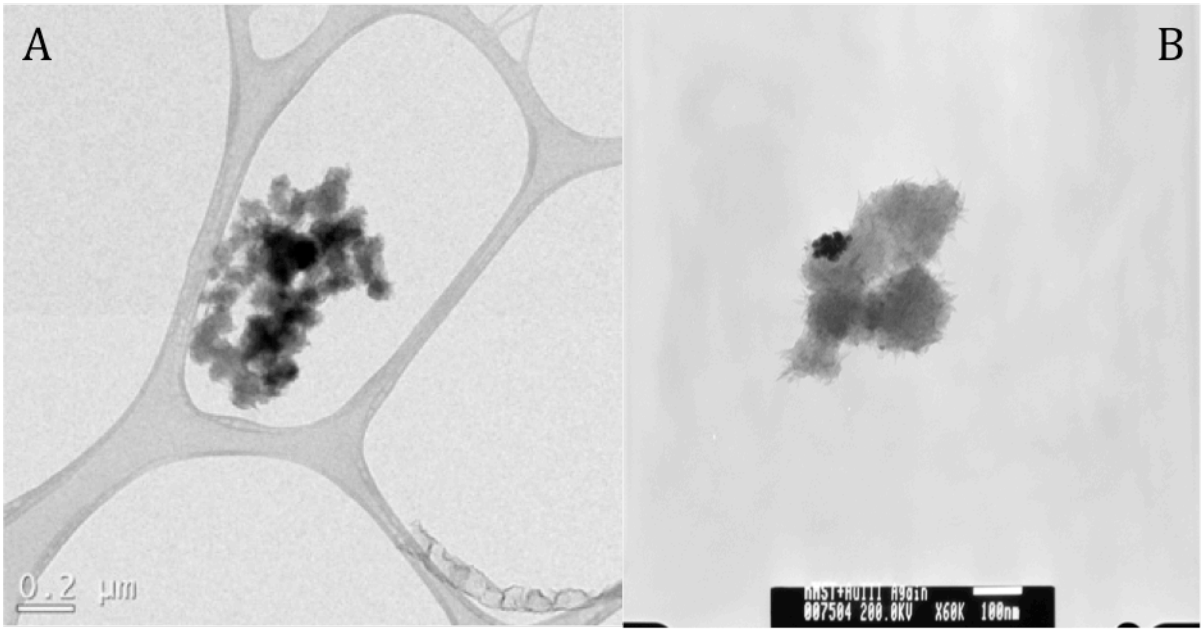

Figure 2.2: TEM images of nMST-Au(III)

A: at concentration of 200 mg/L

B: TEM image of nMST-Au(III) provided by Dr. David Hobbs

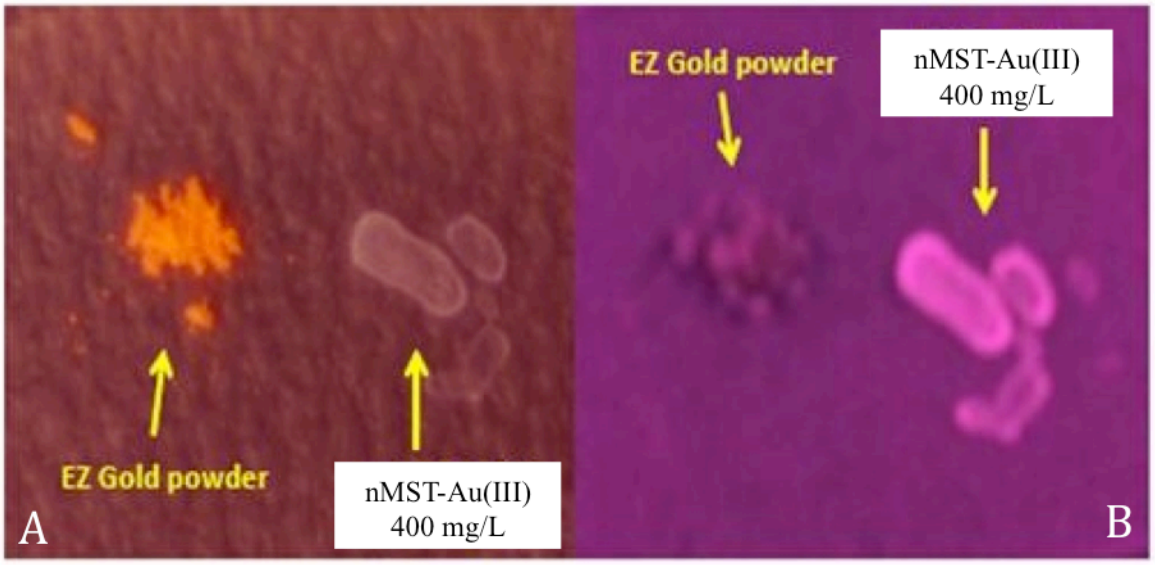

Figure 2.3: Images of 400 mg/L nMST-Au(III)

A. Under flash B. under UV light

CHAPTER 3

ANTIBACTERIAL ACTIVITY OFTITANATES AND GOLD-TITANATES

INTRODUCTION

According to previous studies, OD reading was used to determine bacterial cell number. There was a limitation of using high titanate and metal-titanate concentration with this method because the colloidal characteristic of the titanate interfered with the OD reading (Davis *et al.*, 2007; Chung *et al*., 2011; Drury *et al*., 2014). New methodology that helps examine antibacterial activity of titanates and metal-titanates with the concentration greater than 25 mg/L would be useful. MST and APT with various metal ions were tested against Gram-negative periodontal pathogens such as *A. actinomycetemcomitans*, *P. gingivalis,* and *P. intermedia.* (Chung *et al*., 2011) They found Au(III)-titanates most often inhibited bacterial growth compared to palladium (Pd) or platinum (Pt)-titanates and no antibacterial effects of titanates without metal ions were observed. Therefore, metal-ions play an important role as antimicrobial agents, whereas titanates alone appear to serve as carriers to deliver ions to the target. Gram-positive oral bacteria are important etiological factors in caries formation, but antimicrobial efficacy of gold-titanates against these bacteria is still unknown.

In this study, a method was developed to examine the effect of titanates and gold-titanates at various concentrations against *L. casei* and *S. mutans* by first using bacterial protein as an indicator of total bacterial cell mass. The objective for this specific aim was to determine effects of MST, APT, nanoMST with and without gold particles in different concentrations on bacterial cell mass of three Gram-positive cariogenic bacteria (*S. mutans*, *L. casei*, and *A.*

viscosus) and control Gram-positive non-pathogenic bacterium (*S. gordonii*). Our hypotheses are that only gold-titanates affect Gram-positive cariogenic bacterial cell mass but titanates alone play a role only as carriers and have no antibacterial effect.

MATERIALS AND METHODS

Bacterial Strains

All four bacteria*, A. viscosus*, *L. casei*, *S. gordonii,* and *S. mutans* were grown as described in materials and methods in chapter 2. After overnight culture, each bacterial species was added to new medium combined with different titanates, gold-titanates, sterile water, or erythromycin as described in experimental design below.

Exposure of Titanates or Gold-Titanates to Bacterial Samples

The types of titanates and gold-titanates used in this experiment were MST, APT, nMST, MST-Au(III), APT-Au(III), and nMST-Au(III), provided by Dr. David Hobbs (Savannah River National Laboratory). Total 10^8 CFUs of *L. casei* or *S. mutans* were prepared in 900 µL volume MRS or BHI medium. In each bacterial suspension, 100 µL of stock titanate or gold-titanate solution was added to make up a final concentration of 400, 200, 100, 50, 25, or 10 mg/L in a total 1 mL sample. 100 µL of sterile water and 50 mg/mL erythromycin were used as negative and positive controls, respectively.

Bacterial Protein Extraction and Protein Assay

After 24 h exposure, all cultures were collected for protein assays. B-PER® Bacterial Protein Extraction Reagent (Pierce®, Rockford, IL, USA) was used to extract the bacterial protein. Bacterial protein concentration was measured on the bacterial extract using a BCA

protein assay kit (Pierce®) as per manufacturer's instructions. Bovine serum albumin was used to calibrate the BCA assay. BCA samples were measured at 560nm by using microplate reader (Magellan™, TECAN, San Jose, CA).

Statistical Analysis

In all experiments, the 95% confidence intervals and *p*-values indicate whether the difference is statistically significant. In the preliminary bacterial culture studies, each bacterial species was analyzed separately. After 24 h exposure, all the samples exposed to titanates were assessed whether they differed in average protein concentrations versus the bacterial controls, using Wilcoxon rank-sum tests.

RESULTS

Effect of Gold-Titanates and Titanates on Bacterial Cell Mass

Bacterial protein concentrations of *S. gordonii*, *A.viscosus*, *L. casei*, and *S. mutans* after 24 h exposure to various types of titanate or gold-titanate in different concentrations are shown in Figure 3.1-3.4, respectively. Untreated bacteria-only and erythromycin were used as negative and positive controls, respectively. At any concentration of three gold-titanate groups, *S. gordonii* protein concentrations were decreased when compared to bacteria-only control (*p*-value < 0.001). Total cell mass of *S. gordonii* was decreased by 29% only when concentrations of all three gold-titanates went from 200 to 400 mg/L. For all three titanates-alone groups, no statistical difference of *S. gordonii* protein levels was observed when compared to bacteria-only control (*p*-value > 0.05).

MST and nMST alone had no effect at any concentration on bacterial protein concentrations recovered from *A.viscosus* and *L. casei* at 24 h (Figure 3.2 and 3.3, respectively).

In groups of APT and three gold-titanates, *A.viscosus* protein concentrations were notably decreased when compared to bacteria-only control. Correspondingly, all three gold-titanates and APT significantly decreased *L. casei* cell mass at 24 h when compared to bacteria-only control (p-value < 0.001). At 200 and 400 mg/L nMST-Au(III), *L. casei* protein concentrations were decreased by 29% and 70% respectively, when compared to concentration of 10 mg/L .

However, only two gold-titanates, MST-Au(III) and nMST-Au(III), showed statistically significant changes in *S. mutans* protein concentrations compared to bacteria-only control (p-value < 0.001) (Figure 3.4). Overall, nMST-Au(III) at 400 mg/L was the most effective at reducing bacterial protein levels in all four bacteria.

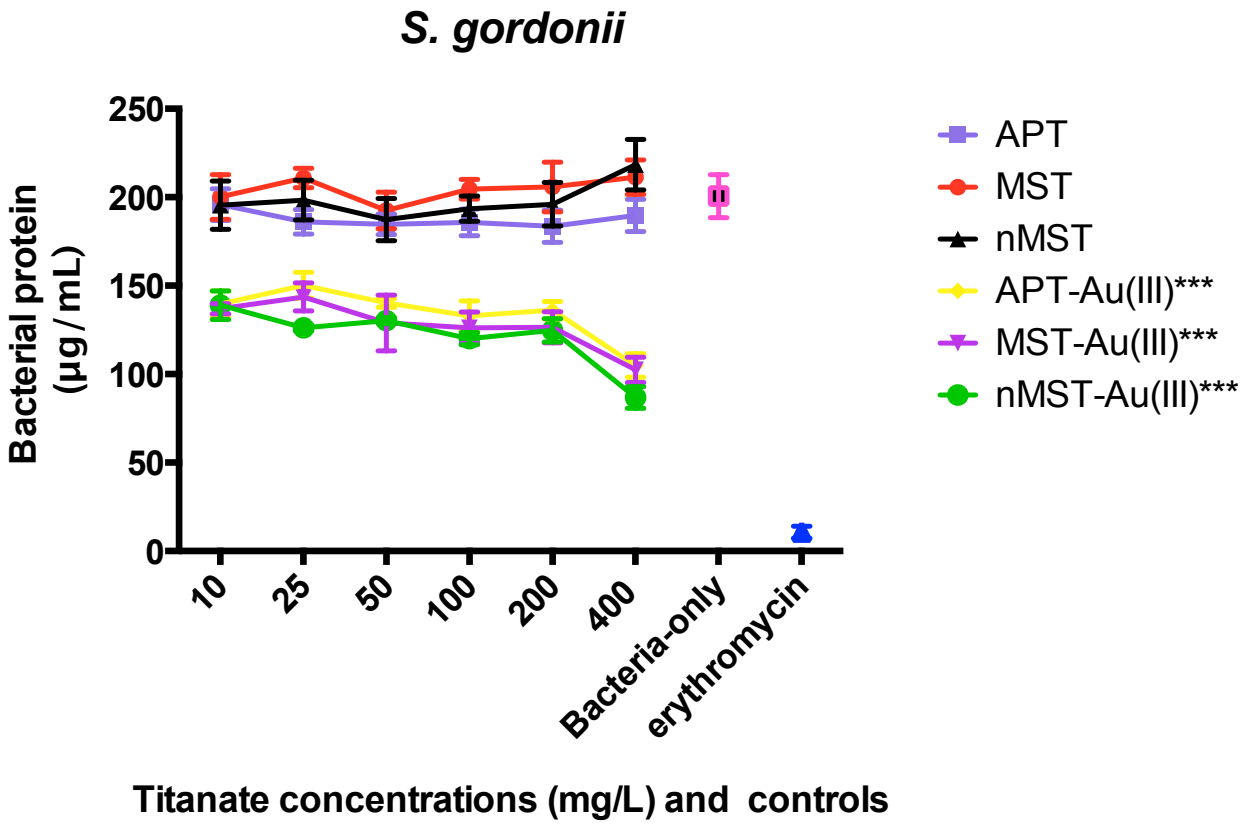

Figure 3.1: This graph illustrates protein concentrations of *S. gordonii* after 24 h exposure to various types of titanate or gold-titanate in different concentrations. Sterile water (H_2O) and erythromycin were used as negative and positive controls, respectively. In each concentration, the means ± standard deviation (SD) of bacterial protein concentrations after treatment with titanates, gold-titanates, or controls were shown. Each titanate or gold-titanate group is represented by different colors. Each concentration is labeled in X-axis.

(***, *p*-value < 0.001)

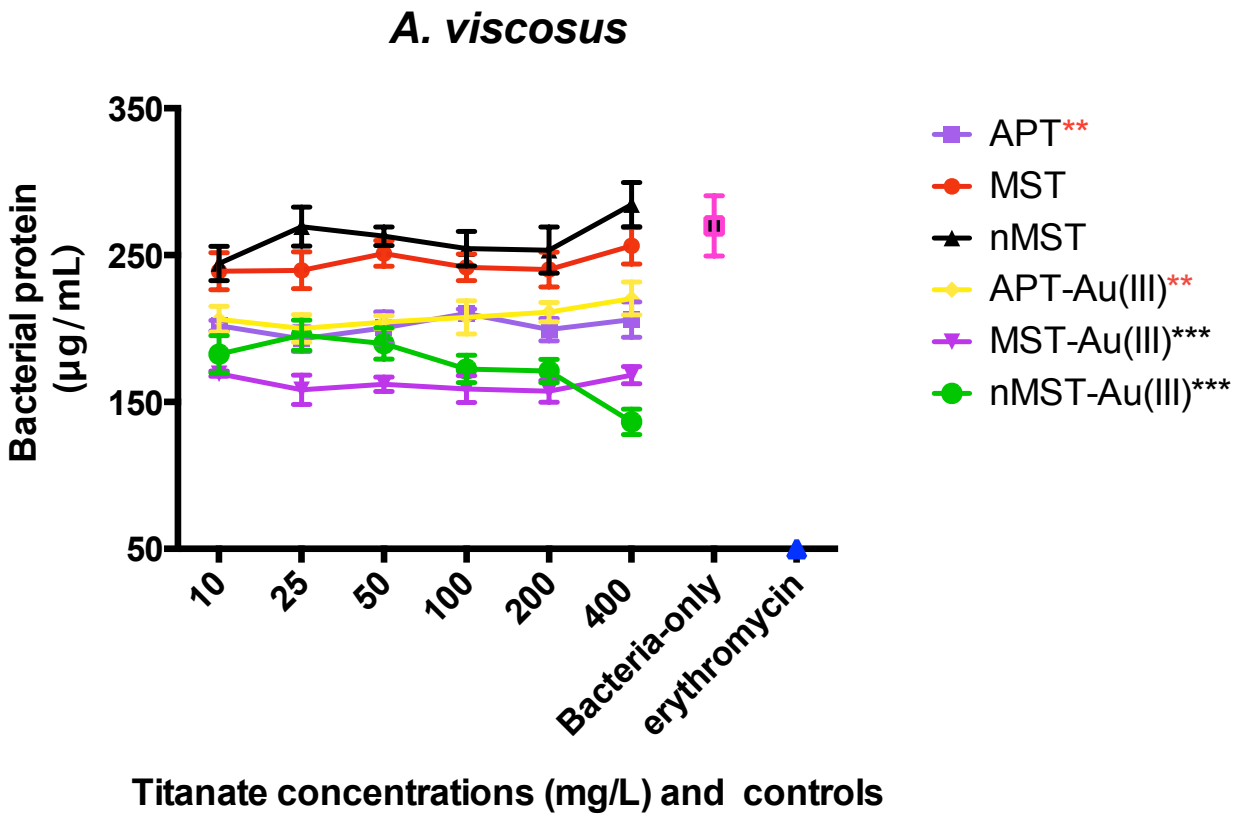

Figure 3.2: This graph illustrates protein concentrations of *A. viscosus* after 24 h exposure to various types of titanate or gold-titanate in different concentrations. Sterile water (H_2O) and erythromycin were used as negative and positive controls, respectively. In each concentration, the means ± standard deviation (SD) of bacterial protein concentrations after treatment with titanates, gold-titanates, or controls were shown. Each titanate or gold-titanate group is represented by different colors. Each concentration is labeled in X-axis.

(**, p-value < 0.01; ***, p-value < 0.001)

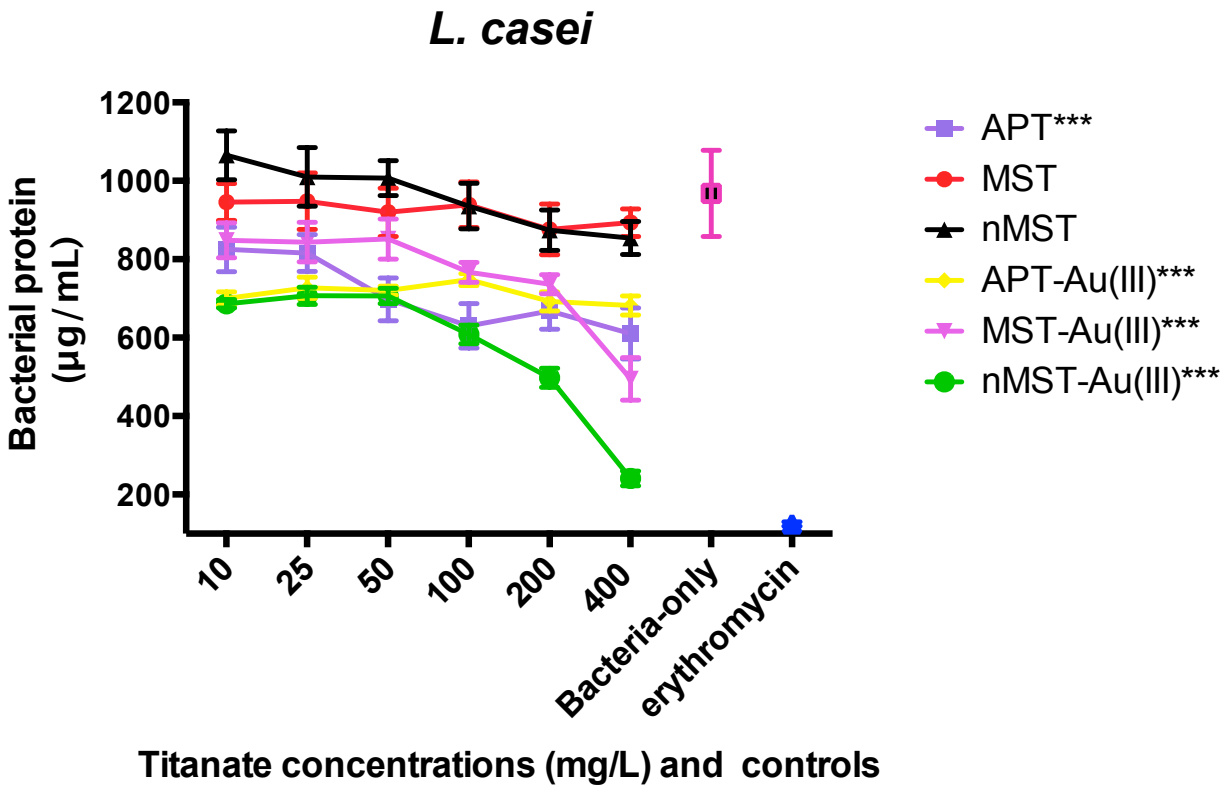

Figure 3.3: This graph illustrates protein concentrations of *L. casei* after 24 h exposure to various types of titanate or gold-titanate in different concentrations. Sterile water (H_2O) and erythromycin were used as negative and positive controls, respectively. In each concentration, the means ± standard deviation (SD) of bacterial protein concentrations after treatment with titanates, gold-titanates, or controls were shown. Each titanate or gold-titanate group is represented by different colors. Each concentration is labeled in X-axis.

(***, *p*-value <0.001)

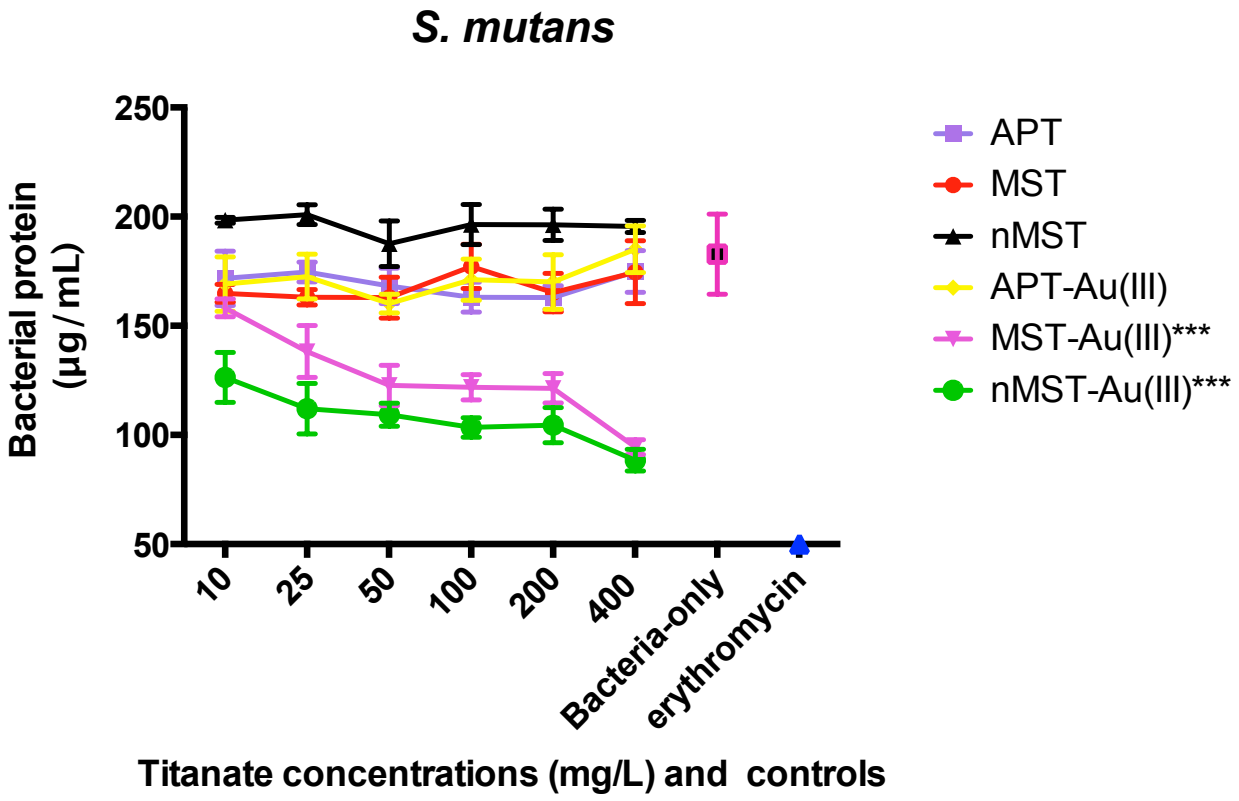

Figure 3.4: This graph illustrates protein concentrations of *S. mutans* after 24 h exposure to various types of titanate or gold-titanate in different concentrations. Sterile water (H_2O) and erythromycin were used as negative and positive controls, respectively. In each concentration, the means ± standard deviation (SD) of bacterial protein concentrations after treatment with titanates, gold-titanates, or controls were shown. Each titanate or gold-titanate group is represented by different colors. Each concentration is labeled in X-axis.

(***, p-value < 0.001)

DISCUSSION

We initially investigated the antimicrobial activity of various types and concentrations of titanates and gold-titanates against Gram-positive cariogenic bacteria. Since determining cell concentration by OD reading had limitation due to the colloidal nature of the added titanates (Chung *et al*., 2011), we determined the total bacteria cell mass based on total bacterial protein. This method eliminated the OD interference issue as well as interference with direct bacterial mass (dry weight) since bacterial protein was extracted and the bacterial pellets with any titanates were discarded before analysis.

L. casei showed highest protein concentrations compared to *S. mutans*, *S. gordonii*, and *A. viscosus*. This is because *L. casei* has a larger cell size that is around 0.7- 1.1 x 2.0- 4.0 micrometers whereas *Actinomyces* are around 0.5 x 1.7-2.9 micrometers and *Streptococci* diameters are around 0.5 micrometers (Whitman *et al*., 2012).

Based on the bacterial protein assay, nMST-Au(III) showed the best effectiveness among titanates and gold-titanates to decrease bacterial protein mass. This may be because of differences among titanates that are carriers to release gold ions to bacterial environment. Nano-size sodium titanate has a smaller size but similar morphology to micron-sized sodium titanates. Consequently, this increases particle surface area, which may help improve its antibacterial activity. In a previous study, AuNPs with various surface modifications and composition showed differential antimicrobial activity against *E. coli* (Zhou *et al.*, 2012). With the same shape and type of AuNPs, a citrate-capping agent increased AuNPs aggregation and reduced the surface area of NPs that interacted with bacterial cells, leading to decreased inhibitory effect. Therefore, increasing the surface area of NPs generates further biophysical interaction between NPs and bacteria. Hernández-Sierra *et al.* (2008) investigated antibacterial activity of silver, zinc oxide

and gold NPs against *S. mutans* and found that AuNPs had an effect on *S. mutans* only at the initial concentration of 197 μg/mL. At lower concentrations, AgNPs showed better antibacterial activity than the other NPs. According to their electron microscopy images, the average size of AgNPs (25 nm) was smaller than AuNPs (80 nm) and zinc oxide NPs (125 nm). This study supports that smaller sized NPs have better interaction with bacterial cells.

However, the protein level could represent either live or dead cells in bacterial suspension so these results were not able to show bacterial viability after exposure to titanate compounds. Consequently, a more definitive study was carried out on *S. mutans* and *L. casei* bacterial growth over time (described in Chapter 4).

In conclusion, gold-titanates showed significant reduction in Gram-positive cariogenic and non-pathogenic bacterial cell protein in the presence of gold-titanates at any concentration. nMST-Au(III) showed considerable inhibition of all four bacterial cell mass and would be a suitable antimicrobial agent against Gram-positive cariogenic bacteria.

CHAPTER 4

DYNAMIC SUSPENDED GROWTH ANALYSIS

INTRODUCTION

Nano-monosodium titanate (nMST) has been introduced as an ion exchanger which can bind with metal ions and acts as a carrier to exchange metal ions to environment. In a previous chapter, we observed gold-titanate particles significantly decreased total Gram-positive cariogenic bacterial protein mass after 24 h exposure. Nano-sized gold-titanate (nMST-Au(III)) appeared to be the most effective particles among the group tested. Thus, a more exhaustive study was carried out in this chapter using nMST-Au(III) only.

Typical bacterial growth in batch culture consists of four characteristic phases. Lag, exponential, stationary, and death phases are recorded as changes in number of viable cells versus time (Figure 4.1). Immediately after inoculation into fresh media, bacteria need time to initially adjust to new conditions, and this time period is called lag phase. During the lag phase, bacteria remain temporarily unchanged. When they start dividing regularly, the numbers of cells increase exponentially by the process of binary fission. Bacterial cells usually divide at a constant rate at this point, which is called exponential (log) phase. This process continues until bacterial growth is limited by either accumulation of inhibitory end products or lack of essential nutrients. At this stage, bacteria stop growing and the number of dividing cells equal the number of cells dying, thus the net accumulation of cells is zero, and cell concentration attains a plateau, which is called stationary phase. After that, bacteria viable cell numbers decline, which is called death phase.

The objective of this study was to quantify the effects of nMST-Au(III) on *S. mutans* and *L. casei* bacterial growth over time by using a Live and Dead (L/D) cell viability analysis and colony forming units. The hypothesis of this aim is that nMST-Au(III) demonstrates antibacterial activity against both *S. mutans* and *L. casei*.

MATERIALS AND METHODS

Bacterial Strains and Gold-titanates

L. casei and *S. mutans* were grown aerobically as pure species in batch suspended growth cultures at 37 °C following the protocol from chapter 2.

nMST-Au(III) concentrations evaluated were 10, 200, and 400 mg/L. Untreated bacteria cells were used as bacteria-only control.

Live/Dead Cell Viability Assay

Bacterial cultures (10^8 CFUs/mL) were exposed to 400, 200, or 10 mg/L of nMST-Au(III) at time=0 of batch suspended cultures. Untreated control cultures for both species were used to establish their normal growth rates. Triplicate samples of cell suspension were collected every two hours from each culture for 16 h. The LIVE/DEAD® BacLight™ Bacterial Viability kit (Molecular Probes®, Eugene, OR) was used to quantify bacterial cell viability. The staining kit is composed of two dyes. Syto9, green fluorescence nucleic acid stain, labels all bacterial DNA. Syto9 has fluorescence excitation/emission at 480/500nm. Propidium Iodide (PI), red fluorescence nucleic acid stain, can only penetrate bacteria with damaged membranes (*i.e.,* 'dead' bacteria), causing a reduction in the Syto9 stain fluorescence intensity. The fluorescence excitation/emission for PI is 490/635 nm. Each stained sample was filtered through a 0.2µm Whatman® Cyclopore® membranes (Sigma-Aldrich®, St. Louis, MO), and mounted onto

standard glass microscope slide for counting. The live and dead cell images were taken on the same field by fluorescence microscope at 100x magnification. Five image sets per sample were taken and counted with ImageJ™ image analysis software (National Institutes of Health (NIH), Bethesda, MD). In Figure 4.2, the images of live and dead cells are shown independently in green and red cells, respectively. After using ImageJ™ image analysis software, live and dead cell images were merged and counted. (Figure 4.3)

Colony Forming Units (CFUs)

Separate *L. casei* and *S. mutans* culture samples were diluted serially with phosphate buffered saline (PBS) and plated onto selective medium agar. Species-specific agar plates, MRS and BHI agars, were used to determine *L. casei* and *S. mutans* CFUs, respectively. All agar plates were incubated aerobically at 37 °C for 24 h. Bacterial colonies were counted and CFUs per volume determined after appropriate dilution factor correction and used as another indicator of viable bacterial cells.

Statistical Analysis

Regarding L/D cell counts and the CFUs in each time point, all three-concentration groups were tested to determine whether the average bacterial cell numbers differed from the untreated control using one-way analysis of variance (ANOVA) and Tukey's multiple comparisons test. The 95% confidence intervals and *p*-values indicate whether the difference is statistically significant.

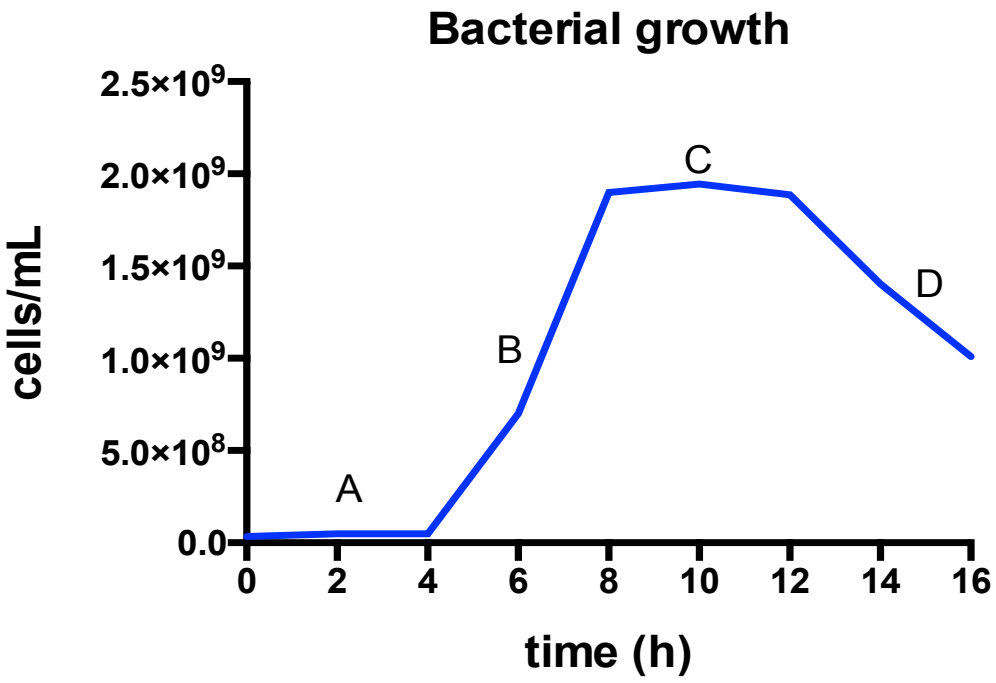

Figure 4.1: Typical bacterial growth in batch culture consists of four characteristic phases: Lag (A), exponential (B), stationary (C), and death (D) phases, recorded as changes in number of viable cells versus time

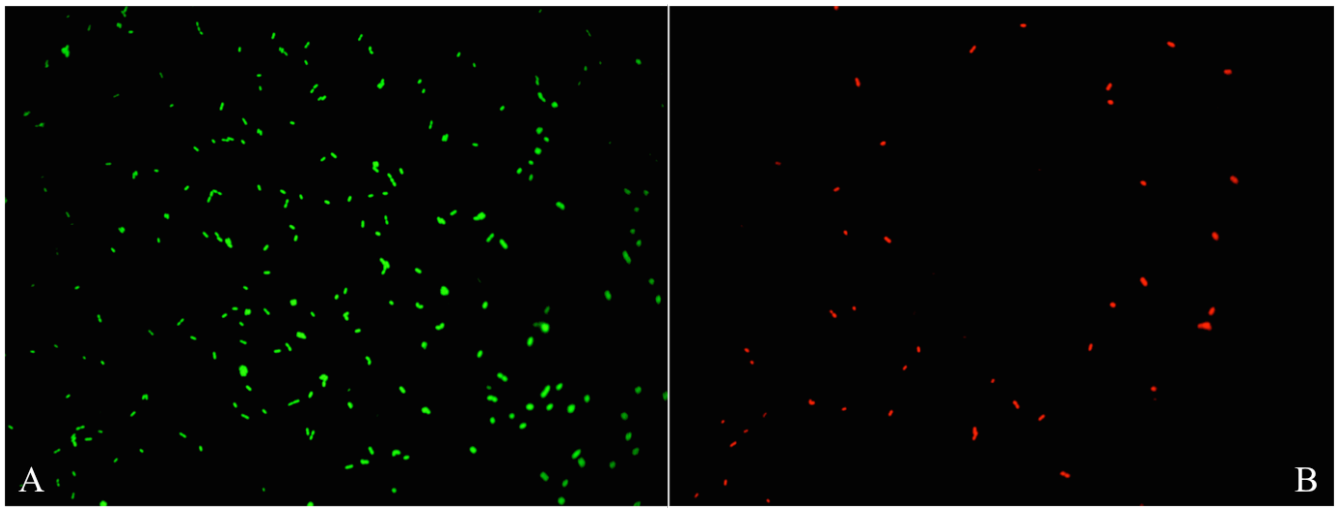

Figure 4.2: Images of untreated *S. mutans* after stained with L/D staining kit at time=0 and taken under fluorescence microscope (100x)

A: Live cells shown in green & B: Dead cells shown in red

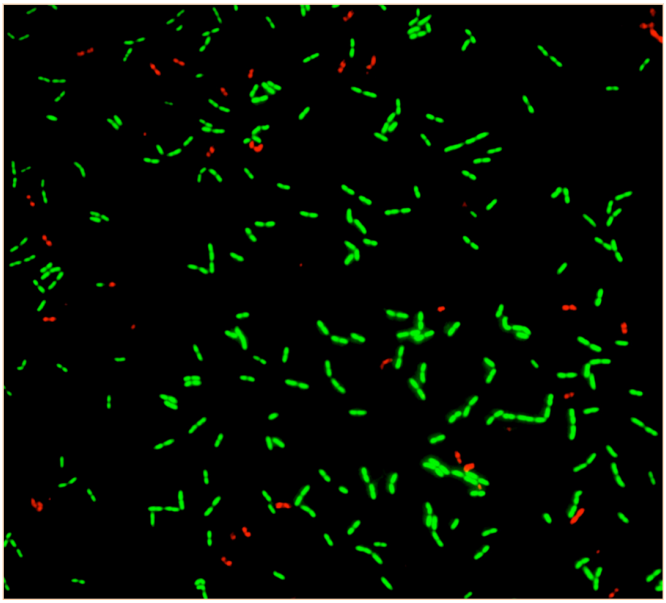

Figure 4.3: Image of live (green) and dead (red) cells of untreated *S. mutans* after stained with L/D staining kit at 4 h, taken under fluorescence microscope (100x), and processed by using ImageJ™ image analysis program

RESULTS

Batch suspended cultures of *L. casei* and *S. mutans* were repeated at varying concentrations of nMST-Au(III) at 37 °C. Liquid samples were collected every two hours for 16 h to determine viable cell counts, either by Live/Dead staining or CFU counts. In the *L. casei* series (Figure 4.4), the low concentration of nMST-Au(III) (10mg/L) had only a marginal effect on the growth rate and growth extent of *L. casei* (p-value<0.05). In Figure 4.4B, the high concentration (400mg/L) of nMST-Au(III) significantly decreased *L. casei* cell numbers as early as 2 h (p-value<0.01). The medium concentration (200mg/L) of nMST-Au(III) also significantly affected *L. casei* growth as early as 6 h, ultimately reducing the numbers of cells at 16 h by a factor of 4x (p-value<0.0001) compared to untreated control cultures.

Unlike *L. casei*, only high and medium concentrations nMST-Au(III) had any effect on *S. mutans* growth (Figure 4.5). At 10 mg/L nMST-Au(III), no significant difference in bacterial growth rate or growth extent compared to the untreated control was found (p-value>0.05). The medium concentration of nMST-Au(III) appeared to have no effect on *S. mutans* growth rate for up to 6 h and only marginally affected the maximum cell numbers attained at 16 h (p-value<0.05). The high concentration of nMST-Au(III) only reduced the maximum cell extent at 16 h by a factor of 2x (p-value<0.001).

Based on CFU cell counts, bacterial growth curves of *L. casei* exposed to the various concentrations of nMST-Au(III) exhibited the same levels of reduction as seen above (Figure 4.6). Conversely, in *S. mutans* CFU study, both 200 and 400 mg/L group similarly affected exponential phase at 4-6 h, which did not correspond with L/D staining study (Figure 4.7).

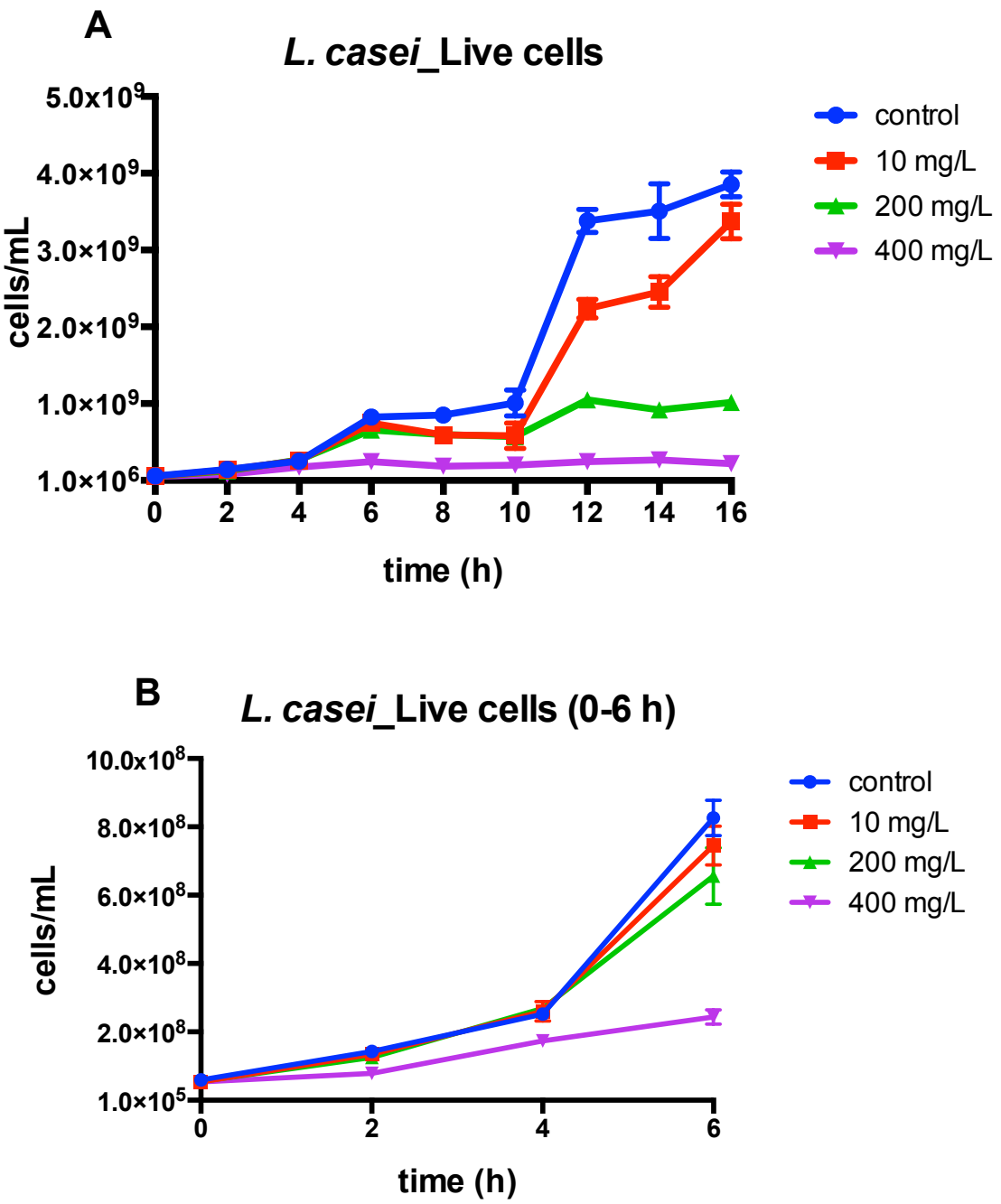

Figure 4.4: The effect of 10, 200, and 400 mg/L (low, medium, and high concentrations) nMST-Au(III) on *L. casei* growth curves at 37 °C over time for (A) all time points (0-16 h) and (B) 0-6 h. All concentrations showed antibacterial activity on *L. casei* growth. High concentration worked as antibacterial agent to totally inhibit *L. casei* at as early as 2 h.

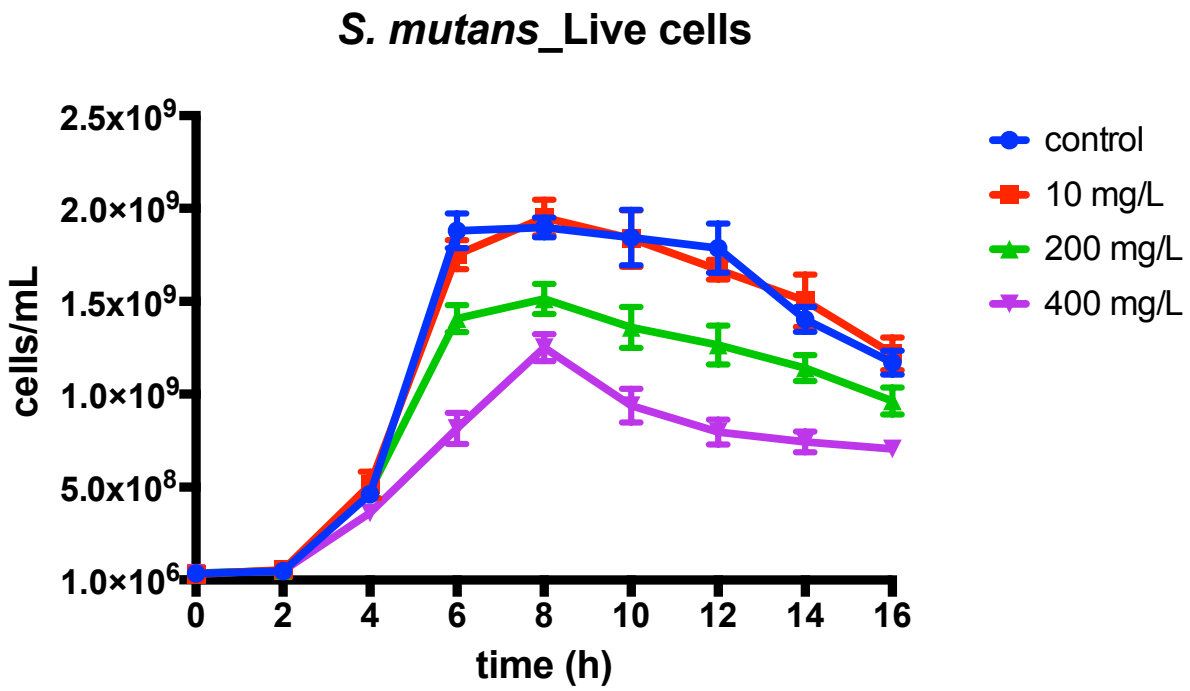

Figure 4.5: The effect of 10, 200, and 400 mg/L (low, medium, and high concentrations) nMST-Au(III) on *S. mutans* growth curves at 37 °C over time. Only medium and high concentrations were able to affect *S. mutans* growth. High concentration had no effect on *S. mutans* cell numbers for up to 6 h.

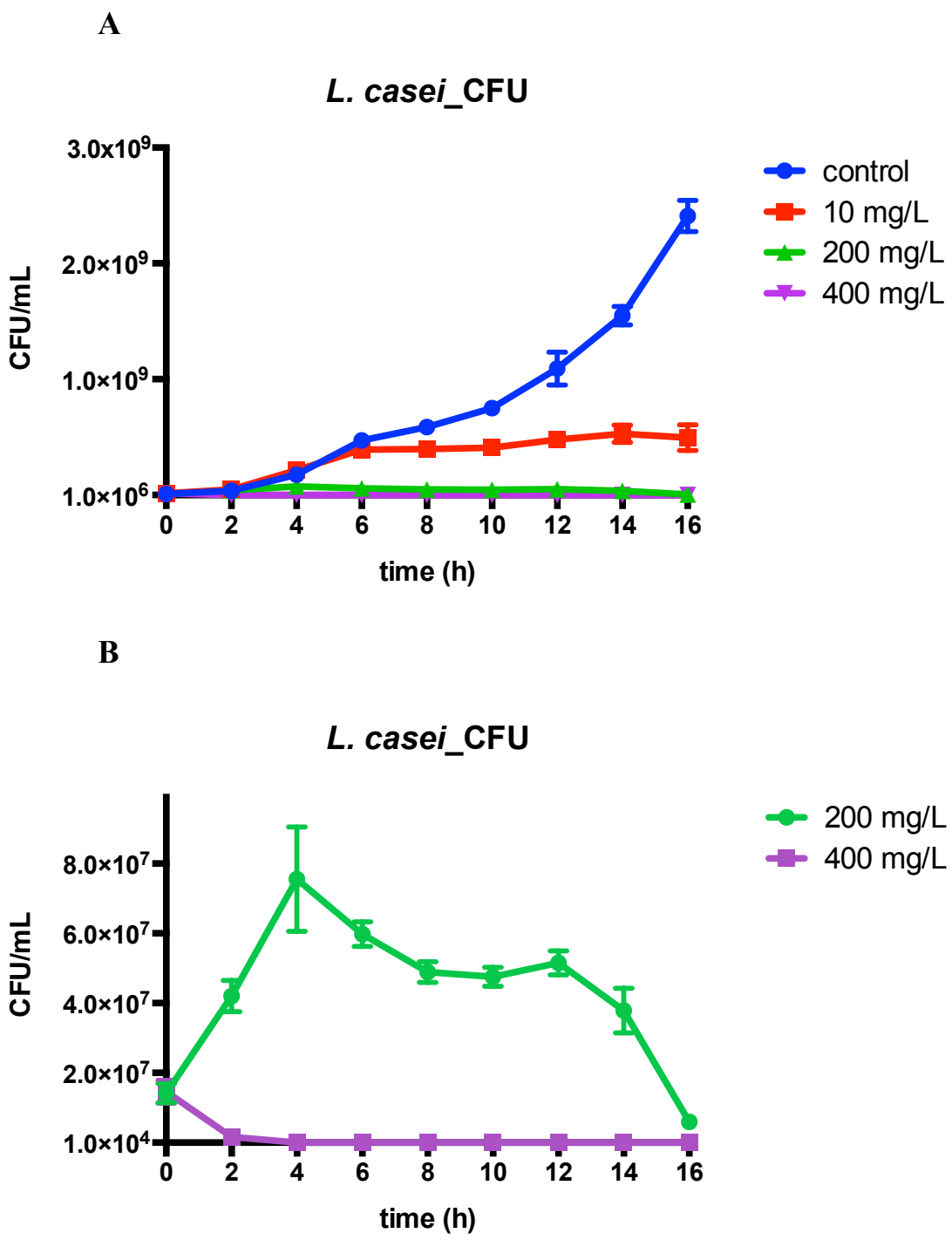

Figure 4.6: The effect of nMST-Au(III) on colony forming units of *L. casei* after 16 h. (A) Untreated control and all three concentrations compared, (B) Only high and medium concentrations compared. All concentrations of nMST-Au(III) showed inhibitory effect on *L. casei* growth. High concentration was the most effective concentration against *L. casei* growth and affected lag phase.

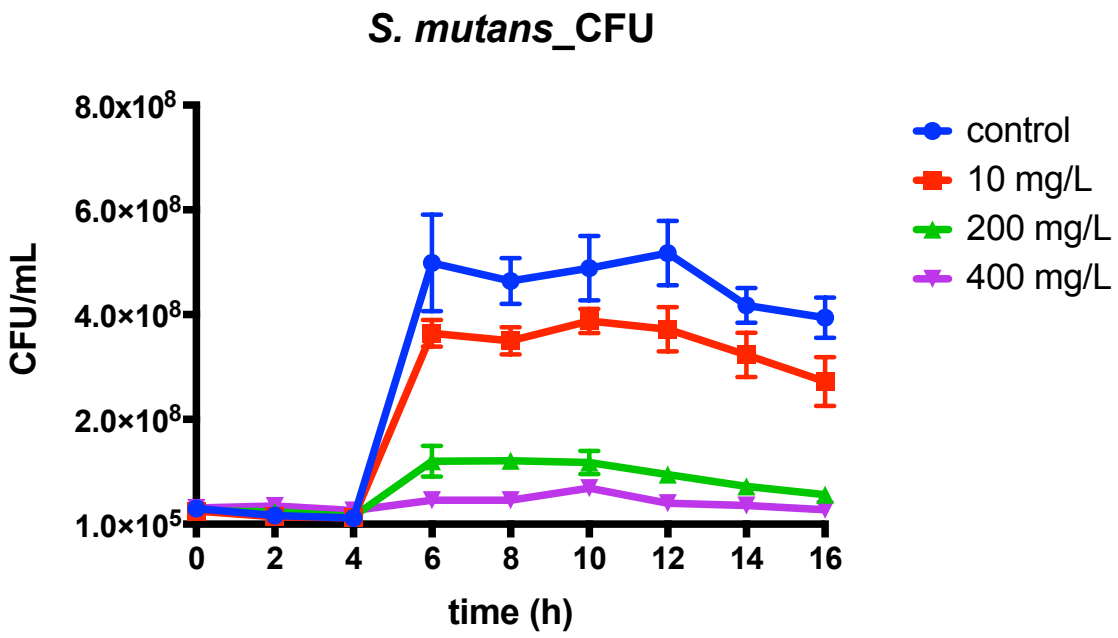

Figure 4.7: The effect of nMST-Au(III) on colony forming units of *S. mutans* after 16 h. High concentration is the most effective concentration against *S. mutans* growth curve.

DISCUSSION

According to the protein assay in chapter 3, nMST-Au(III) caused dramatically significant decrease on all four bacteria protein mass. However, the protein level would represent either live or dead cells in bacterial suspension so the results would not explain if the bacteria were killed or merely suppressed after exposure to titanate compounds. In order to better address this question, L/D staining was used to determine the number of live and dead cells as a function of time in a batch growth culture exposed to different concentrations of nMST-Au(III).

Titanates can bind with several metal ions, and in the present study, gold-titanates were focused to assess their antibacterial activity against Gram-positive cariogenic bacteria. AuNPs were discovered many years ago and the antimicrobial activity of these particles has been studied in both Gram-positive and Gram-negative bacteria such as *Staphylococcus aureus*, *E. coli,* and *Pseudomonas aeruginosa* (Zhao *et al.*, 2010; Brown *et al.*, 2012; Zhou *et al.*, 2012). AuNPs have been recommended for use in different biomedical applications such as labeling and imaging, clinical diagnostics, and therapeutics, since AuNPs present more biocompatibility and less toxicity than other nanoparticles (Boisselier and Astruc, 2009). Kovvuru *et al*. (2014) found AgNPs induced irreversible DNA damage and alteration of genome in mice after a short-term oral exposure, which may cause cancer. Thus toxicity of NPs to mammalian cells is an important factor to consider in potential applications of NPs.

According to this study, *L. casei* appeared more sensitive to nMST-Au(III) than *S.mutans*. Bacterial species may have varied defense mechanisms responding to external stimuli. Overall CFU results corresponded with L/D assay. Unlike L/D staining, low concentration (10 mg/L) of nMST-Au(III) showed antibacterial effect on *S.mutans* exponential phase while no significant difference in activity was seen between low concentration and control on *S.mutans*

cell numbers in L/D staining. Most likely the residual gold-titanate particles on agar may have affected bacterial growth since titanates cannot be separated from the bacterial suspension before adding to agar plates.

Based on these data, we suggest that antibacterial activity of gold-loaded on nano-sized sodium titanate depends on several factors: type, size and surface modification of NPs as well as bacteria species. The mechanism of how nanoparticle work should be further studied to better understand the function of nMST-Au(III)'s effect on these cariogenic bacteria.

In conclusion, nMST-Au(III) did demonstrate antimicrobial activities against *S. mutans* and *L. casei* growth at elevated concentrations of ≥ 200 mg/L.

CHAPTER 5

TRANSMISSION ELECTRON MICROSCOPY

INTRODUCTION

Electron microscopy has been used in many areas to explore nano-scale subjects including cellular structures. Microscopic observation of bacteria has been introduced not only for diagnostic purposes but also for research. Scanning electron microscopy is a powerful technique to observe samples with high resolution and large depth of field. However, it has a limitation when looking into several intracellular structures (Bergmans *et al*., 2005). Transmission electron microscopy (TEM) has been commonly used to investigate intracellular structures of eukaryotic and prokaryotic cells, including bacteria. Many studies used TEM to investigate bacterial structure after exposure to antibacterial agents (Zhao *et al*., 2010; Wang *et al*., 2011). TEM tomography has been developed to construct three-dimensions (3D) nanometer-scaled image (Jinnai *et al*., 2012). TEM tomography can be referred to as a 3D imaging technique that records a series of projection images of a structure from different projection angles and subsequently computes the reconstruction of that structure from these images. TEM tomography also reduces sample preparation time since it does not require embedding and sectioning steps because it can take images in different angles and construct 3D images by computer software. Computer sectioning of the image would show the relationship between the bacterial cell and location of particles. However, conventional TEM has been commonly used to study bacterial structures and would be an alternative choice to investigate our samples, since their embedding and thin-sectioning steps would help reduce the overlapping issues among

bacterial structures and make well-defined images to comprehend intracellular bacterial structures.

In this study, conventional TEM and TEM tomography were used to investigate structures of normal bacteria and after exposure to gold-titanates. According to previous chapters, nano-sized gold-loaded monosodium titanate particles (nMST-Au(III)) dramatically affected *S. mutans* and *L. casei* growth in batch culture but the mechanism of nMST-Au(III) action has not been determined. Therefore, the objective of this chapter is to determine the effect of nMST-Au(III) on three Gram-positive cariogenic bacteria (*S. mutans*, *L. casei*, and *A. viscosus*) and non-pathogenic bacteria (*S. gordonii*) using both conventional TEM and TEM tomography techniques to locate nMST-Au(III). The hypothesis is that gold particles from nMST-Au(III) interact with bacterial structures including bacterial cell wall as well as intracellular bacterial structures.

MATERIALS AND METHODS

Tomographic Transmission Electron Microscopy

S. mutans, S. gordonii, L. casei, and *A. viscosus* were grown as described in materials and methods in chapter 2.

For the preliminary TEM study, tomographic TEM was performed on *S. mutans* and *L. casei*, exposed to 200mg/L nMST-Au(III) or sterile water as controls for 24 h. After getting the preliminary TEM images, exposure time and concentration of nMST-Au(III) were changed to 16 h and 400 mg/L, which followed L/D staining experimental design. All four bacteria, *S. mutans, S. gordonii, L. casei,* and *A. viscosus* were treated with 400 mg/L nMST-Au(III) for 16 h.

Each *S. mutans*, *L. casei*, *S. gordonii* and *A. viscosus* bacterial suspension with new medium (10^8 CFUs/mL) was treated with 400 mg/L nMST-Au(III) or sterile water as controls. After incubation, the bacterial sample preparation protocol from Zhoa *et al*. (2010) was modified to prepare for TEM. Bacteria were washed with phosphate buffer saline (PBS) two times in-between a centrifugal supernatant [3000rpm] for 5 min. Bacterial pellets were removed from suspension by centrifugation. Bacterial pellets were fixed in 2.5% glutaraldehyde solution for 3 h and washed with PBS and then stained with 0.1% Osmic acid for 30 min at room temperature. The bacterial pellets were serially dehydrated in ethanol (EtOH) mixture (v/v, in water) up to 100% EtOH. Each bacterial sample was diluted 1:5 in 100% EtOH. A hundred microliters of each diluted bacterial sample was added to TEM copper grids with a lacy carbon film (Electron Microscopy Sciences, Hatfield, PA), then evaporated slowly under vacuum desiccator for 1 minute and kept in a container with desiccants until TEM images were taken. All sample images were taken on a TEM tomography machine (Model: G2 F20 S Twin, FEI Tecnai™). The experiments were repeated two times independently.

Conventional Transmission Electron Microscopy

All four bacterial samples, *S. mutans, S. gordonii, L. casei,* and *A. viscosus*, were exposed to 400 mg/L nMST-Au(III) for 16 h and then were prepared similarly to the above procedure for tomographic TEM. Thereafter, each bacterial pellet was embedded in epoxy resin and thin-sectioned with microtome. Each sectioned sample was 1x1 millimetre (mm) and 80 nanometres (nm). Each sample was deposited on TEM copper grids with a lacy carbon film (Electron Microscopy Sciences, Hatfield, PA), stained again with Reynold's lead citrate for 10 min, and washed with sterile water.

Samples of nMST-Au(III) for TEM imaging were prepared by slow evaporation of nMST-Au(III) suspension on TEM copper grids with a lacy carbon film (Electron Microscopy Sciences) at room temperature. All bacteria and gold-titanate samples were examined with TEM (JEM-1230, JEOL, Tokyo, Japan). The experiments were repeated two times independently.

RESULTS

Tomographic TEM

In preliminary data with 200mg/L nMST-Au(III) group, TEM images showed nMST-Au(III) mostly attached to the cell walls of *L. casei* and *S. mutans* (Figure 5.1 and 5.2). Images illustrated the overlapping of the particles and the bacteria but particles seem to be outside of the cells. However, this could not be definitely concluded from only these pictures that the particles were just outside the cells.

Changing to the high concentration (400 mg/L) of nMST-Au(III) for 16 h, all four bacterial were investigated. At high concentration (400mg/L), we observed there were more dead bacterial cells than previous TEM images of 200 mg/L nMST-Au(III). These results correspond with L&D staining results, which showed high concentration of nMST-Au(III) has better antibacterial activity against *S. mutans* and *L. casei* growth when compared to medium or low concentration. The spatial location of nMST-Au(III) was confirmed using 3D TEM tomographic technique. In all bacterial TEM images, nMST-Au(III) particles were located at bacterial cell wall and inside bacterial cells (Figure 5.3-5.6). However, overlapping of these particles and bacterial cells could happen. Series images at different angles of TEM were taken. In *S. mutans* and *S. gordonii* images, the particles appeared to be only outside the bacterial cells (Figure 5.7-5.8). These images show nothing conclusive.

Conventional TEM

TEM images of an interaction between nMST-Au(III) and all cariogenic bacteria, *S. mutans*, *L. casei*, and *A.viscosus* (Figures 5.9-5.11) or non-pathogenic bacteria, *S. gordonii* (Figure 5.12) were taken.

Images from conventional TEM disclosed many dead bacteria in nMST-Au(III)-treated samples and relatively few dead bacteria were found in untreated controls. All four bacterial controls showed correct cell morphology and sizes as described in Table 2.1, Chapter 2. Regarding the treated groups, small black particles were observed on bacterial cell walls and were internalized into all four bacteria. Partial rupture of *S. mutans* cell wall showed leakage of bacterial organelles with these particles included (Figure 5.13).

TEM images of nMST-Au(III) in suspension were also taken to compare AuNPs on nMST and black particles that were observed in treated groups (Figure 5.14). We found that AuNPs on nMST have similar size, shape, and density to particles that were inside and attached to bacterial cell wall. These would suggest the particles that were internalized and attached to bacterial cell wall are AuNPs from nMST-Au(III) compound.

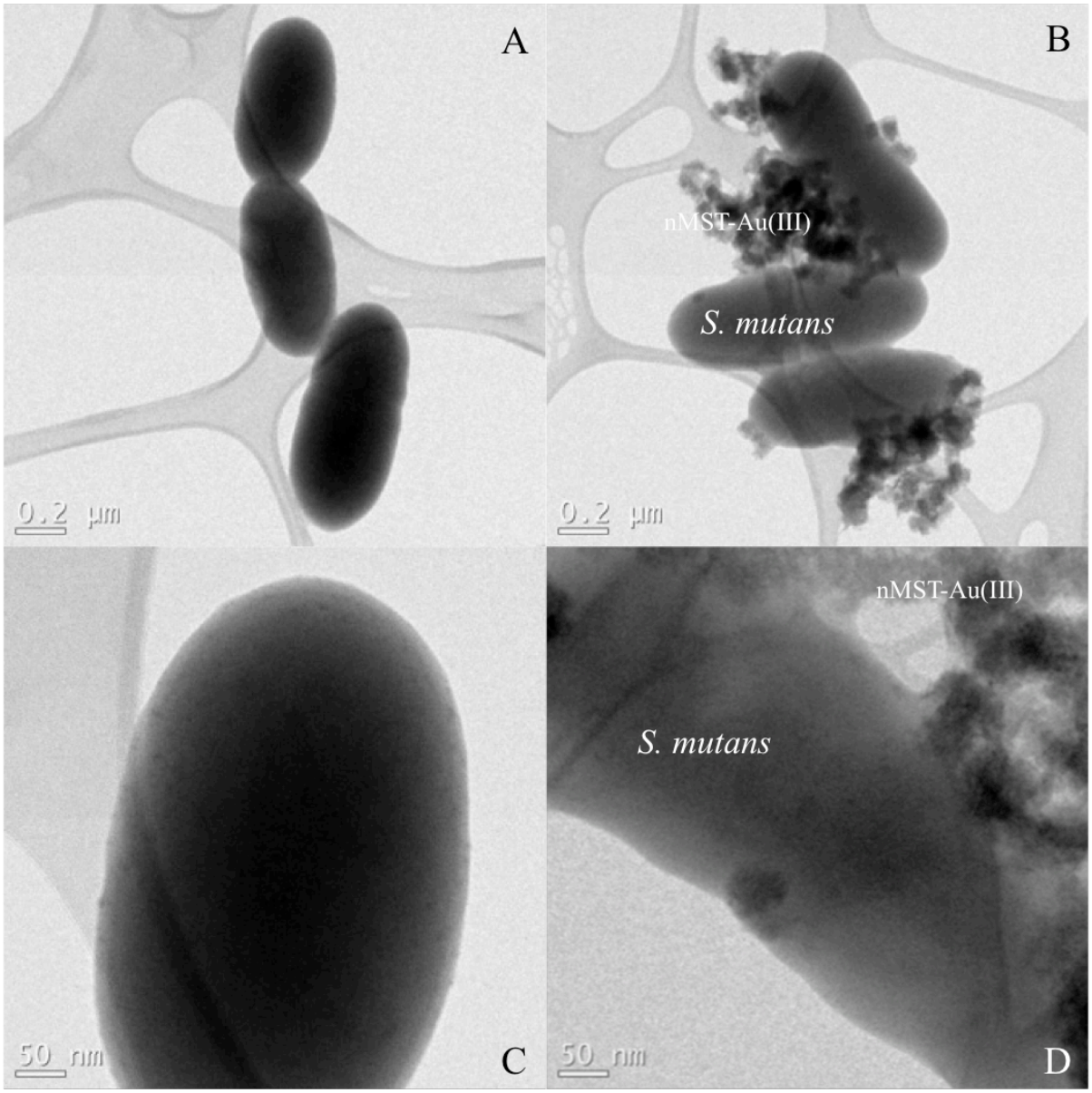

Figure 5.1: Tomographic TEM images of *S. mutans*.

A&C: Bacterial control

B&D: Bacteria after exposure to 200 mg/L nMST-Au(III) for 24 h

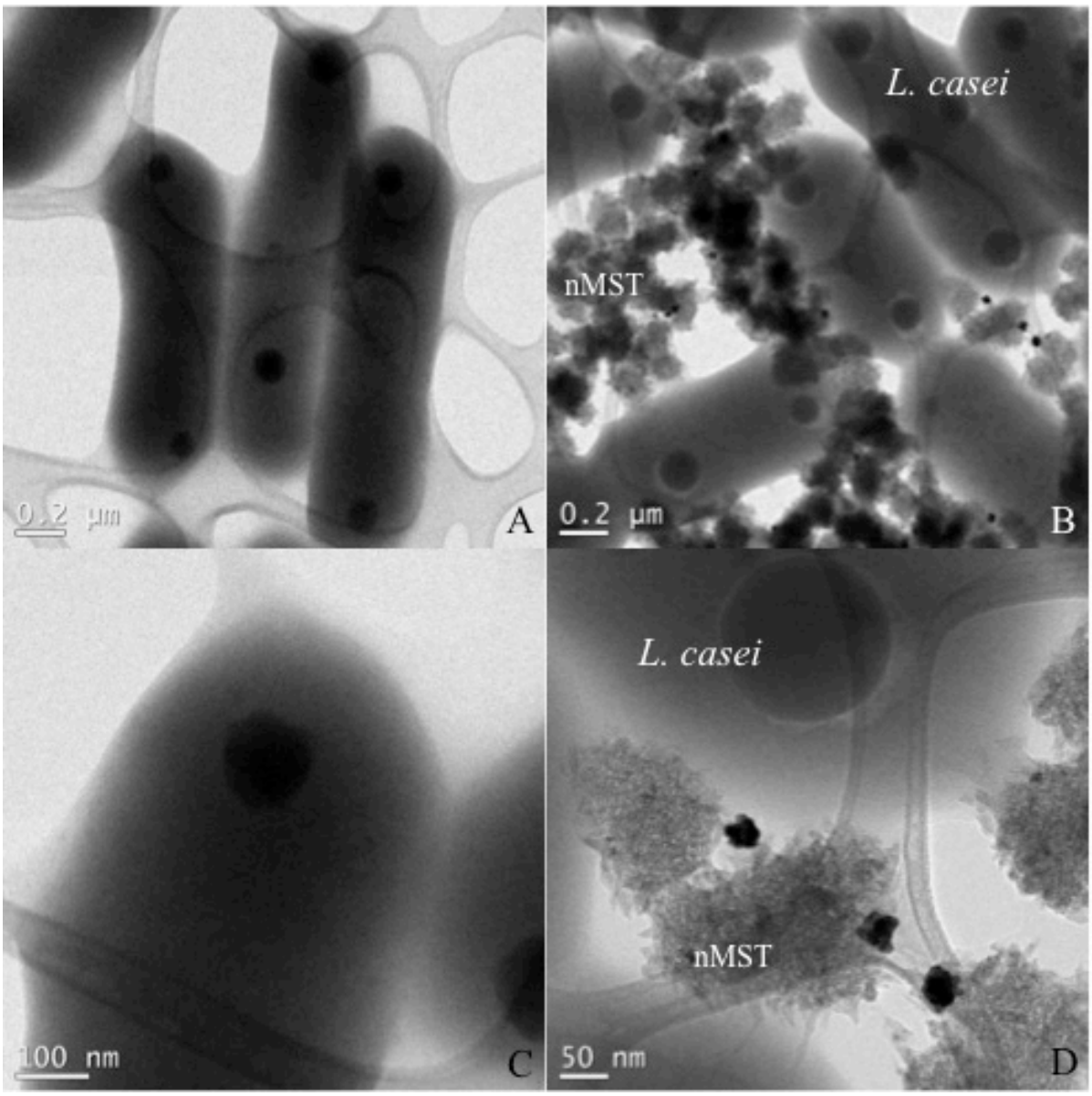

Figure 5.2: Tomographic TEM images of *L. casei.*

A&C: Bacterial control

B&D: Bacteria after exposure to 200 mg/L nMST-Au(III) for 24 h

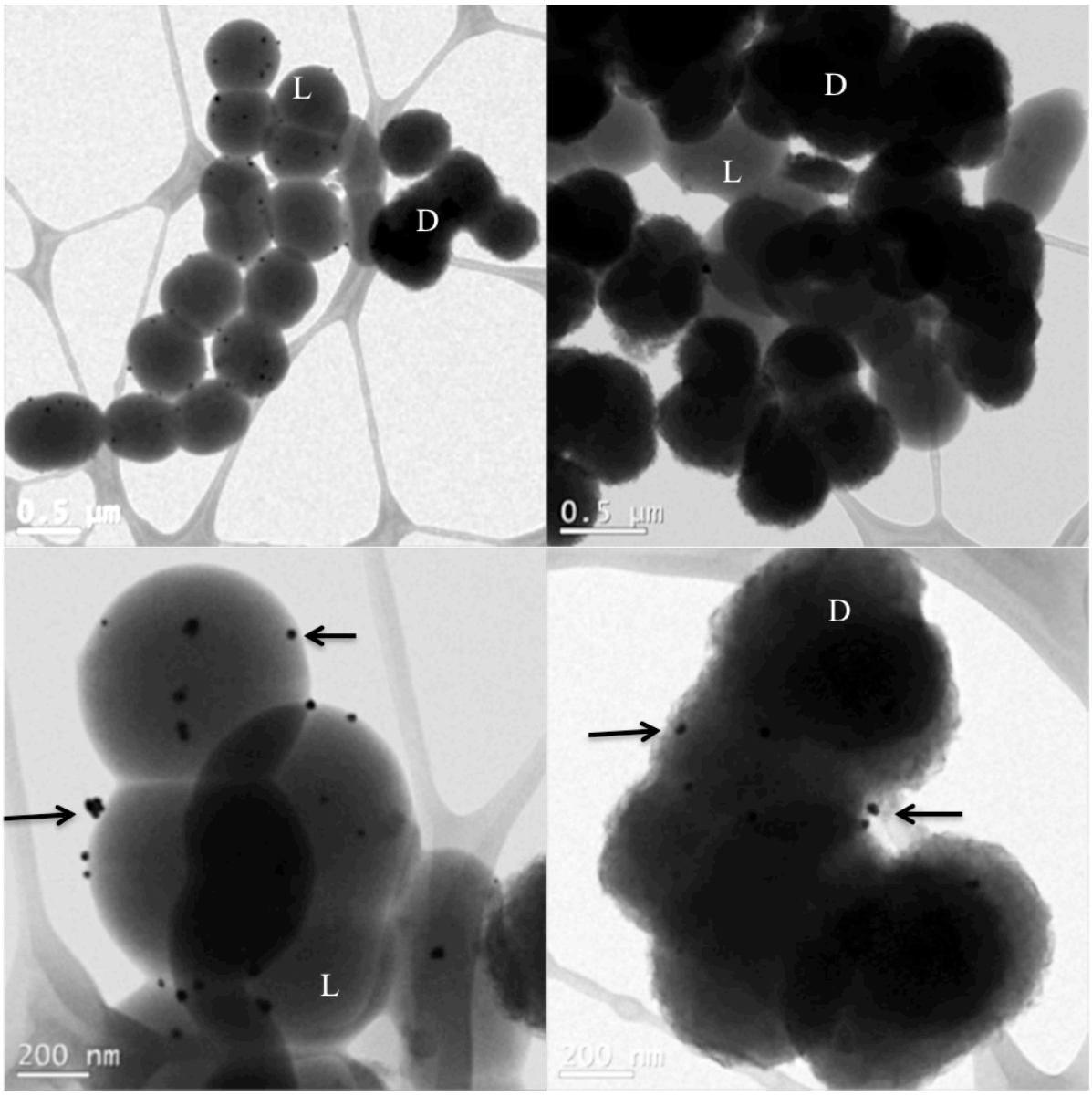

Figure 5.3: Tomographic TEM images of *S. mutans* with 400 mg/L nMST-Au(III) after 16 h exposure, arrows point particles attach to both live (L) and dead (D) cells

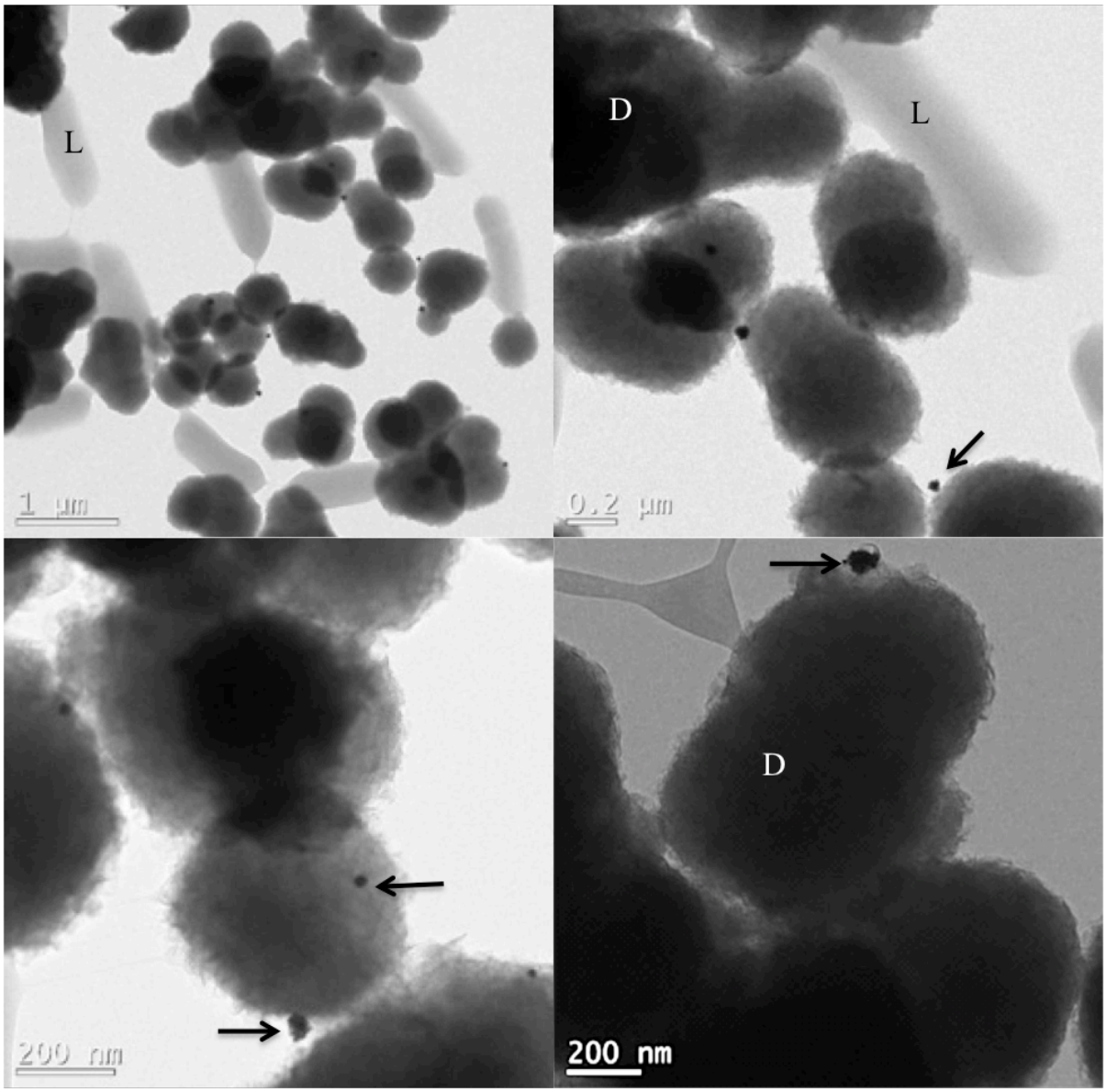

Figure 5.4: Tomographic TEM images of *L. casei* live (L) and dead (D) cells with 400 mg/L nMST-Au(III) after 16 h exposure, arrows point particles attach to dead cells

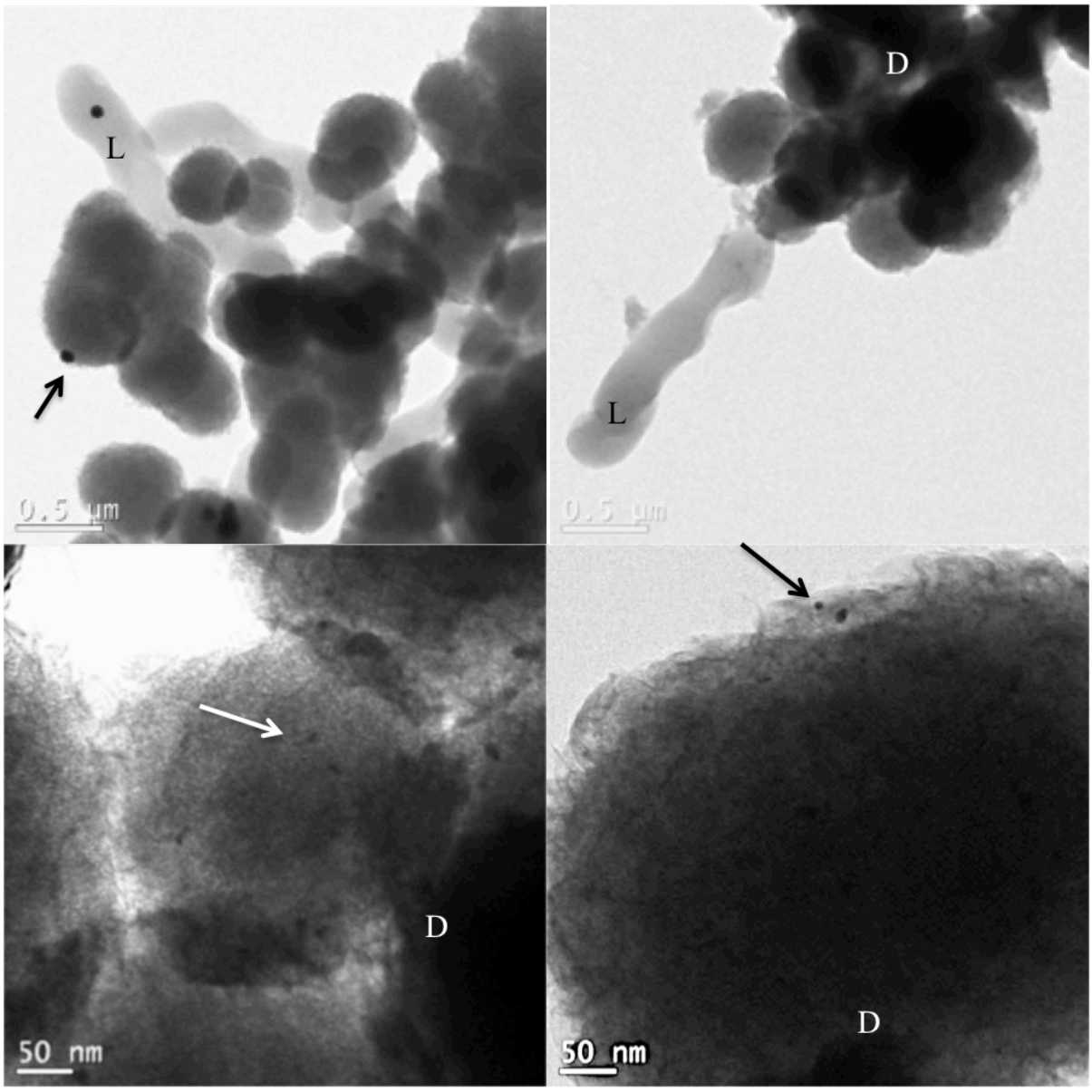

Figure 5.5: Tomographic TEM images of *A. viscosus* live (L) and dead (D) cells with 400 mg/L nMST-Au(III) after 16 h exposure, arrows point particles attach to dead cells

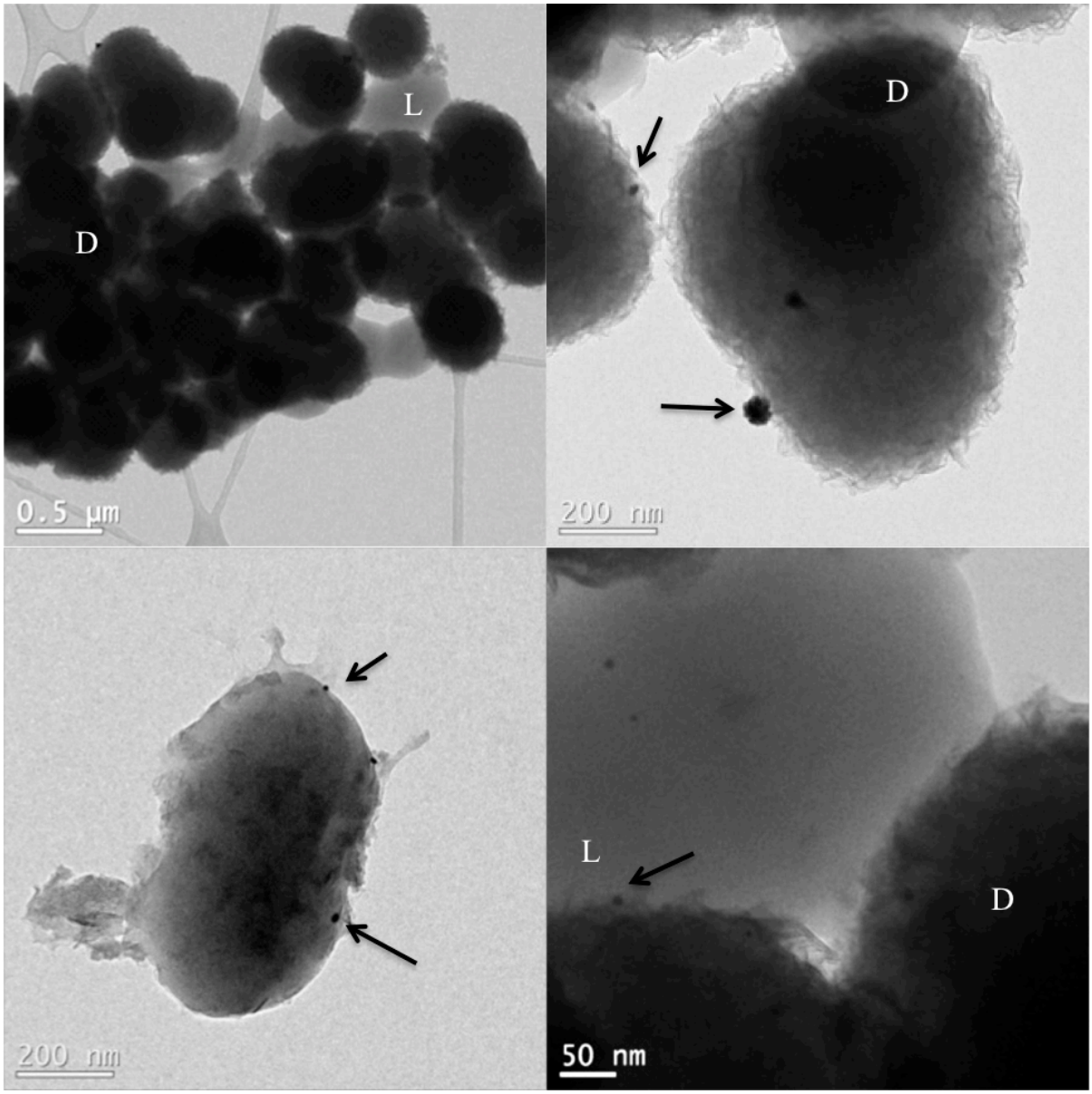

Figure 5.6: Tomographic TEM images of *S. gordonii* live (L) and dead (D) cells with 400 mg/L nMST-Au(III) after 16 h exposure, arrows point particles attach to dead cells

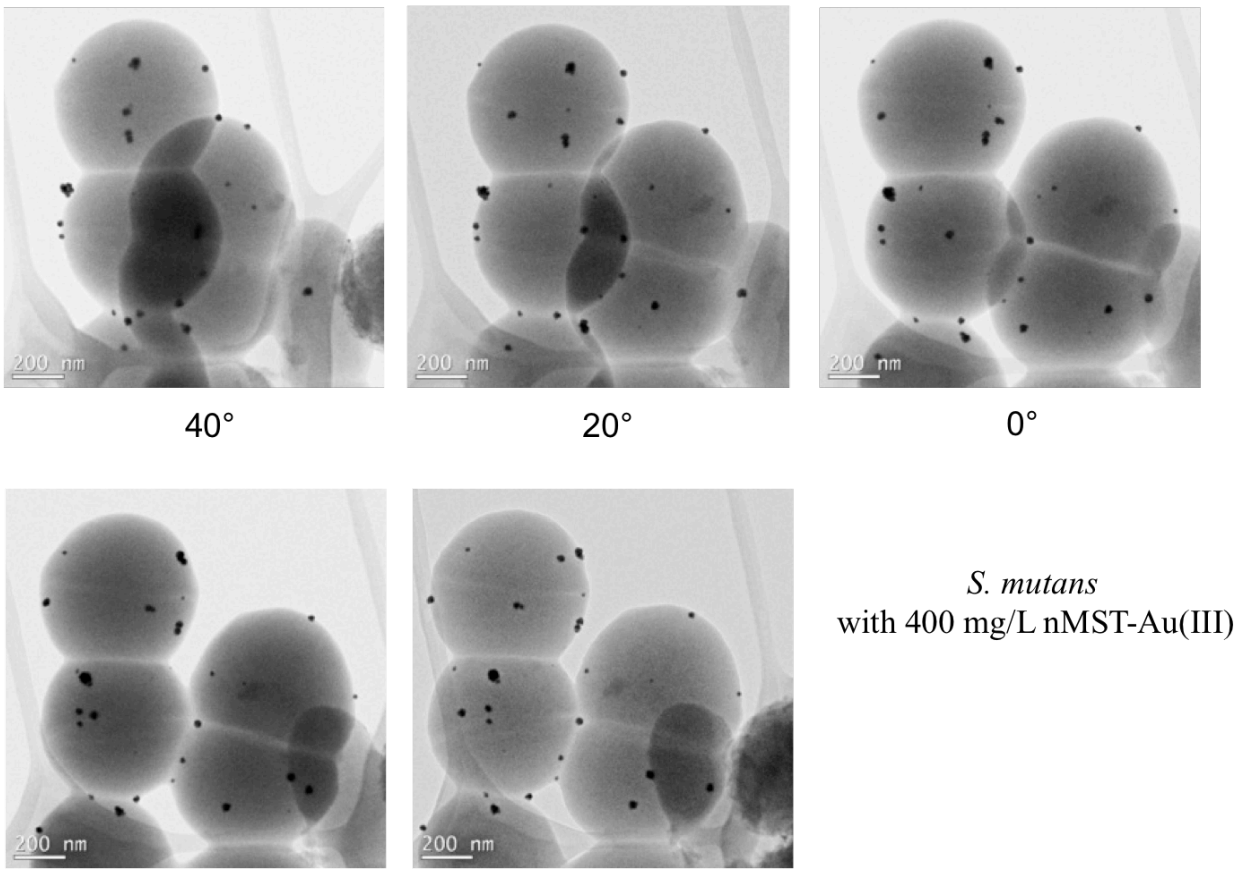

Figure 5.7: Tomographic TEM images of *S. mutans* with 400 mg/L nMST-Au(III) after 16 h exposure, at different angles

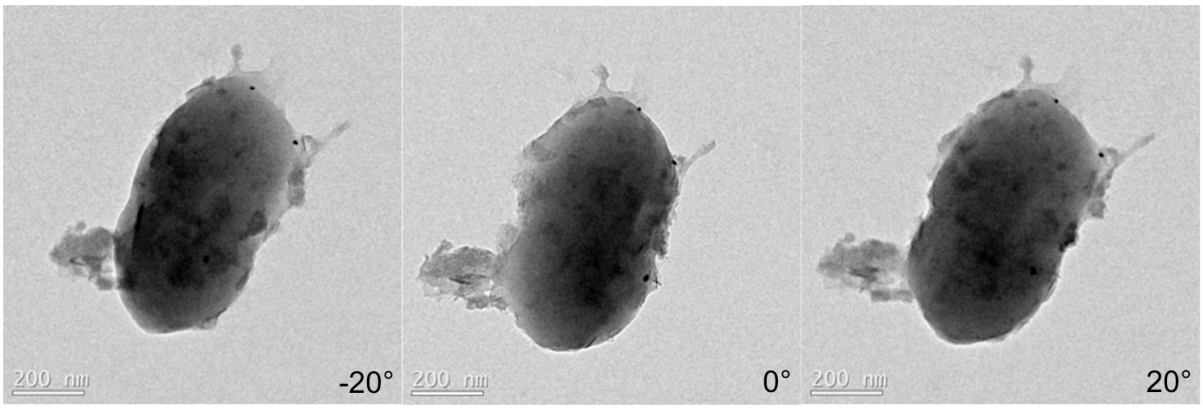

Figure 5.8: Tomographic TEM Images of *S. gordonii* with 400 mg/L nMST-Au(III) after 16 h exposure, at different angles

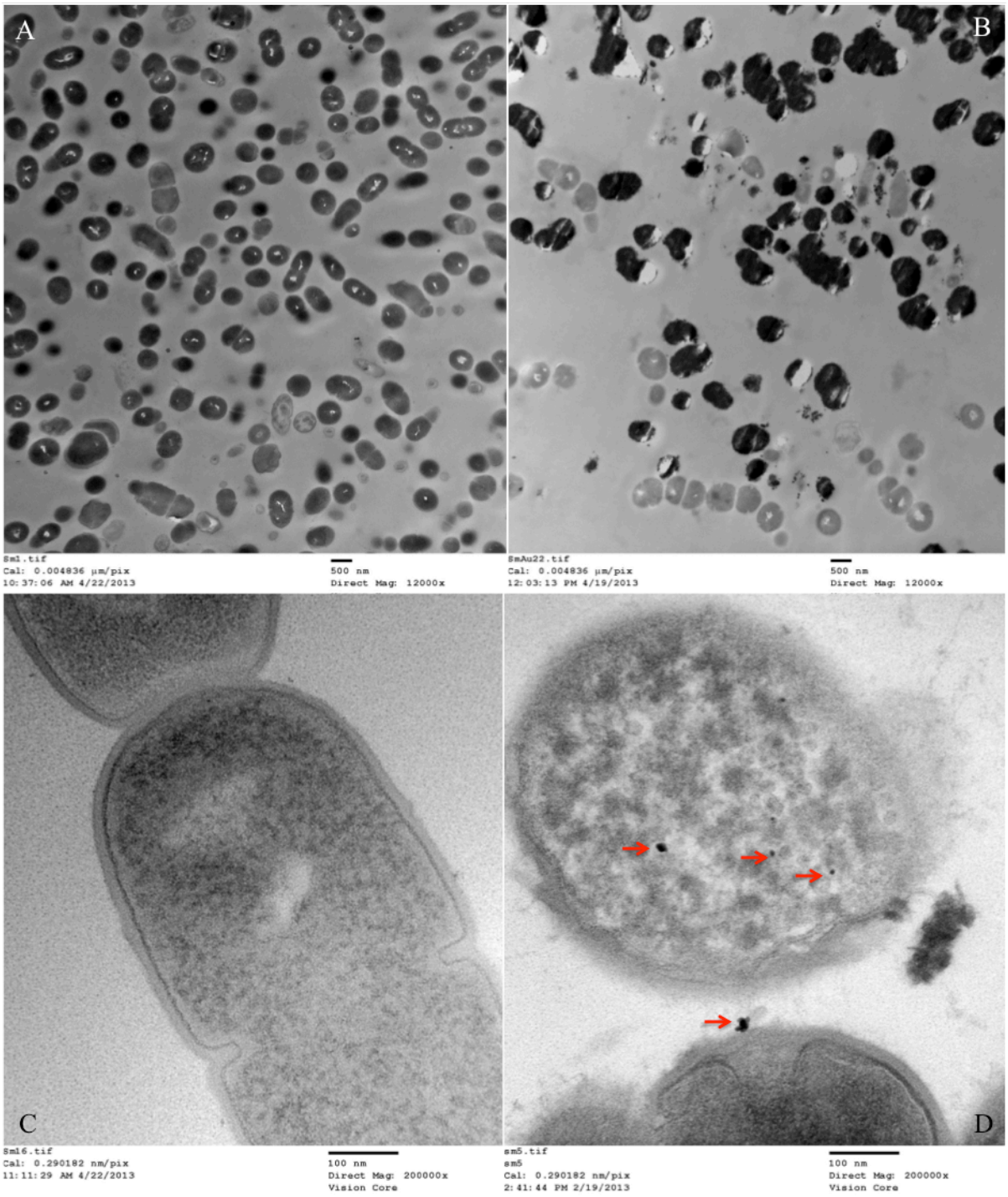

Figure 5.9: Conventional TEM images of *S. mutans*. (A)&(C) Untreated *S. mutans* images taken at magnification 12000X and 120000X, respectively. (B)&(D) *S. mutans* with nMST-Au(III) images taken at magnification 12000X and 120000X, respectively. Arrows point at the nanoparticles (NPs) that were attached to bacterial cell wall and internalized into bacterial cytoplasm.

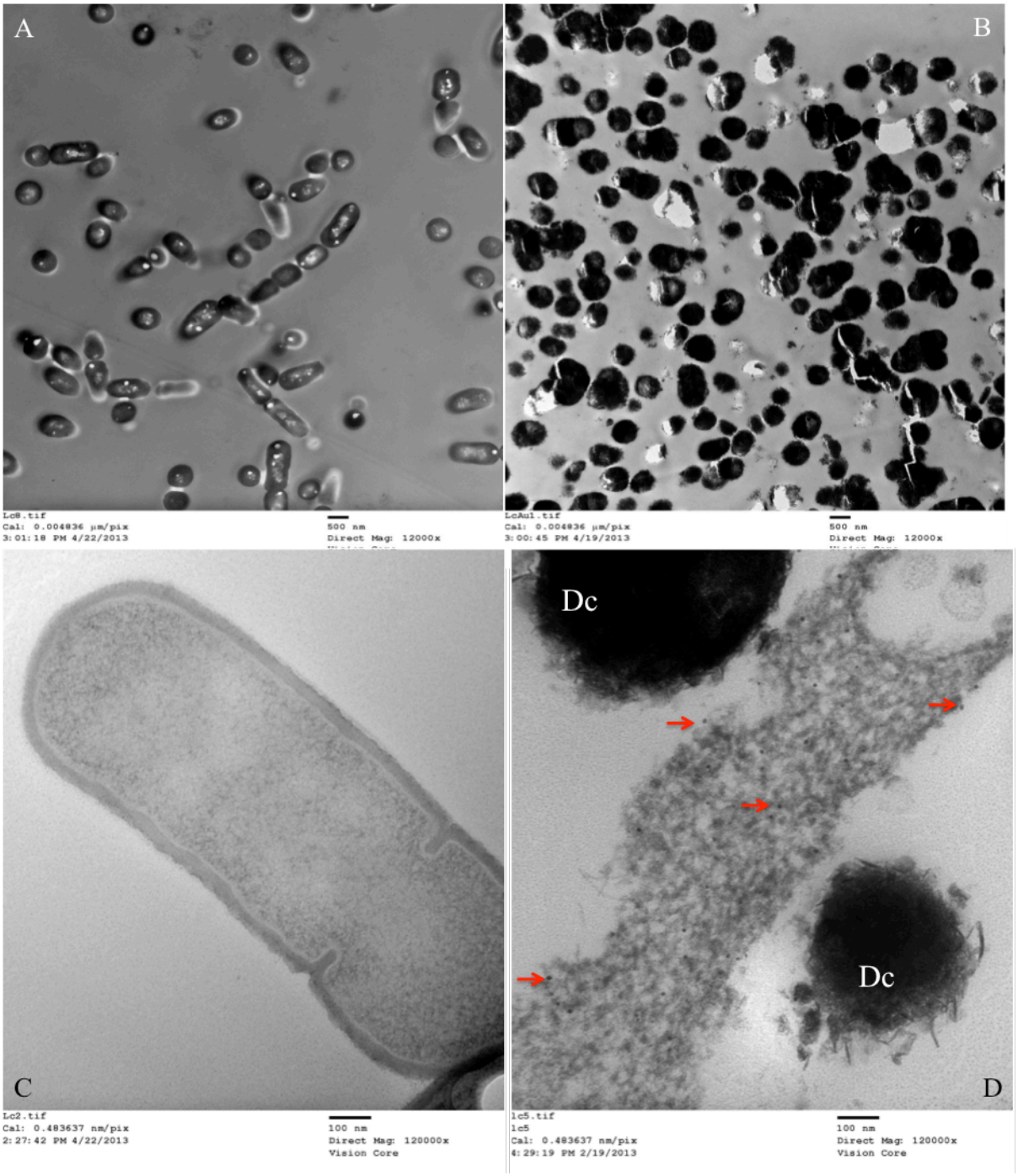

Figure 5.10: Conventional TEM images of *L. casei.* A&C Untreated *L. casei* images taken at magnification 12000X and 120000X, respectively. B&D *L. casei* with nMST-Au(III) images taken at magnification 12000X and 120000X, respectively. Arrows point at the particles that were attached to bacterial cell wall and internalized into bacterial cytoplasm. Dc (dead cells)

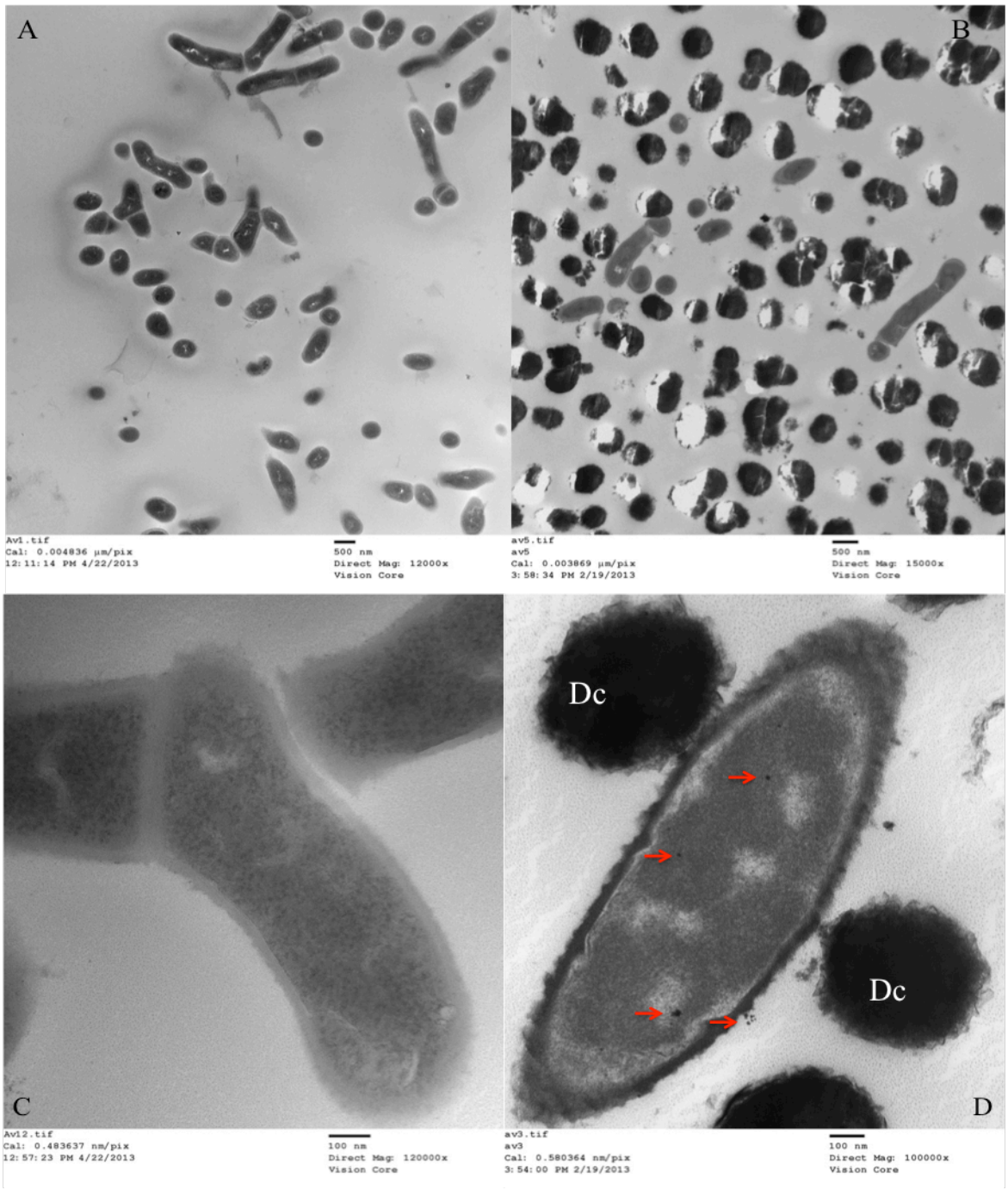

Figure 5.11: Conventional TEM images of *A. viscosus.* A&C Untreated *A. viscosus* images taken at magnification 12000X and 120000X, respectively. B&D *A. viscosus* with nMST-Au(III) images taken at magnification 12000X and 100000X, respectively. Arrows point at the particles that were attached to bacterial cell wall and internalized into bacterial cytoplasm. Dc (dead cells)

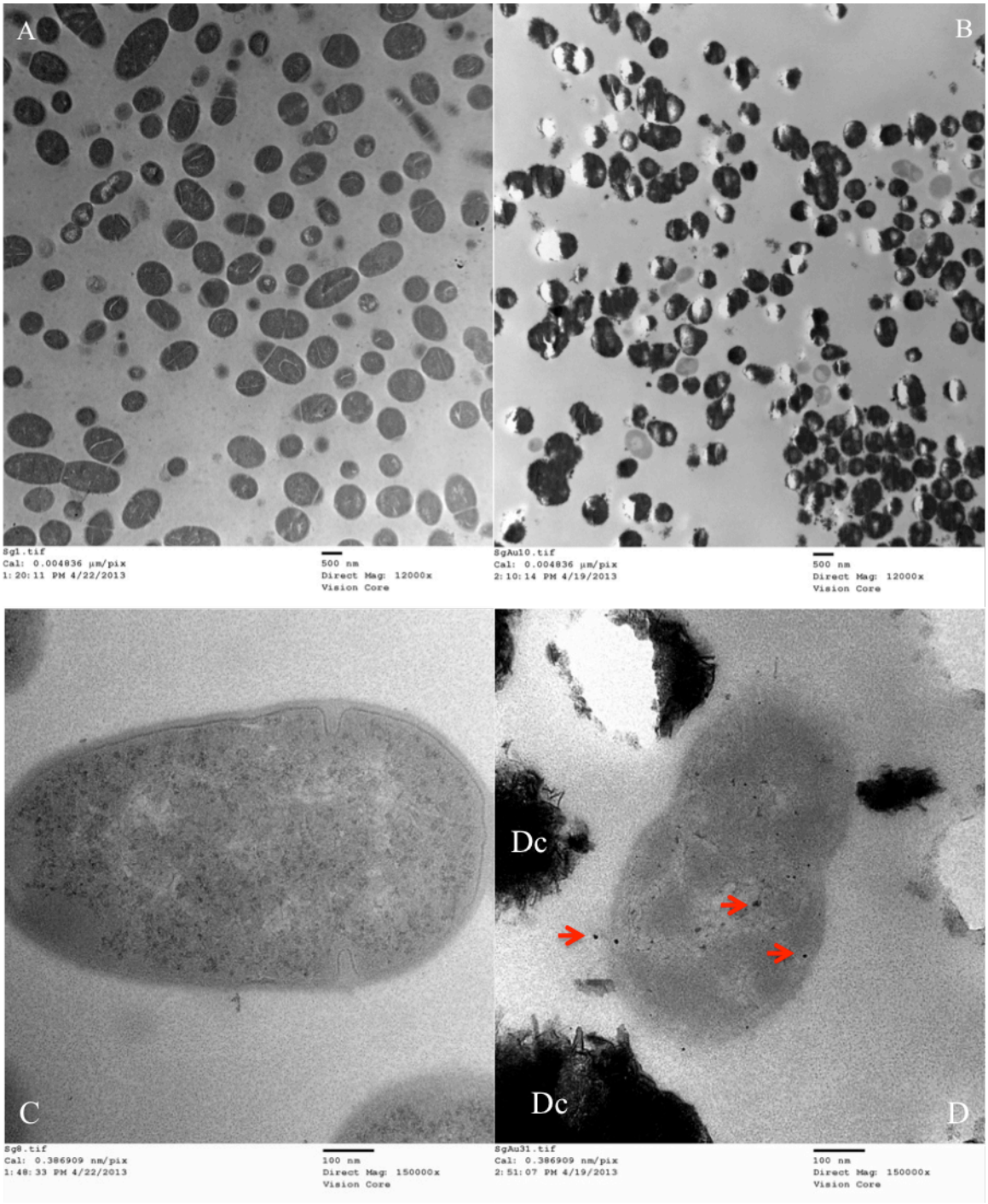

Figure 5.12: Conventional TEM images of *S. gordonii*. A&C Untreated *S. gordonii* images taken at magnification 12000X and 150000X, respectively. B&D *S. gordonii* with nMST-Au(III) images taken at magnification 12000X and 150000X, respectively. Arrows point at the particles that were attached to bacterial cell wall and internalized into bacterial cytoplasm. Dc (dead cells)

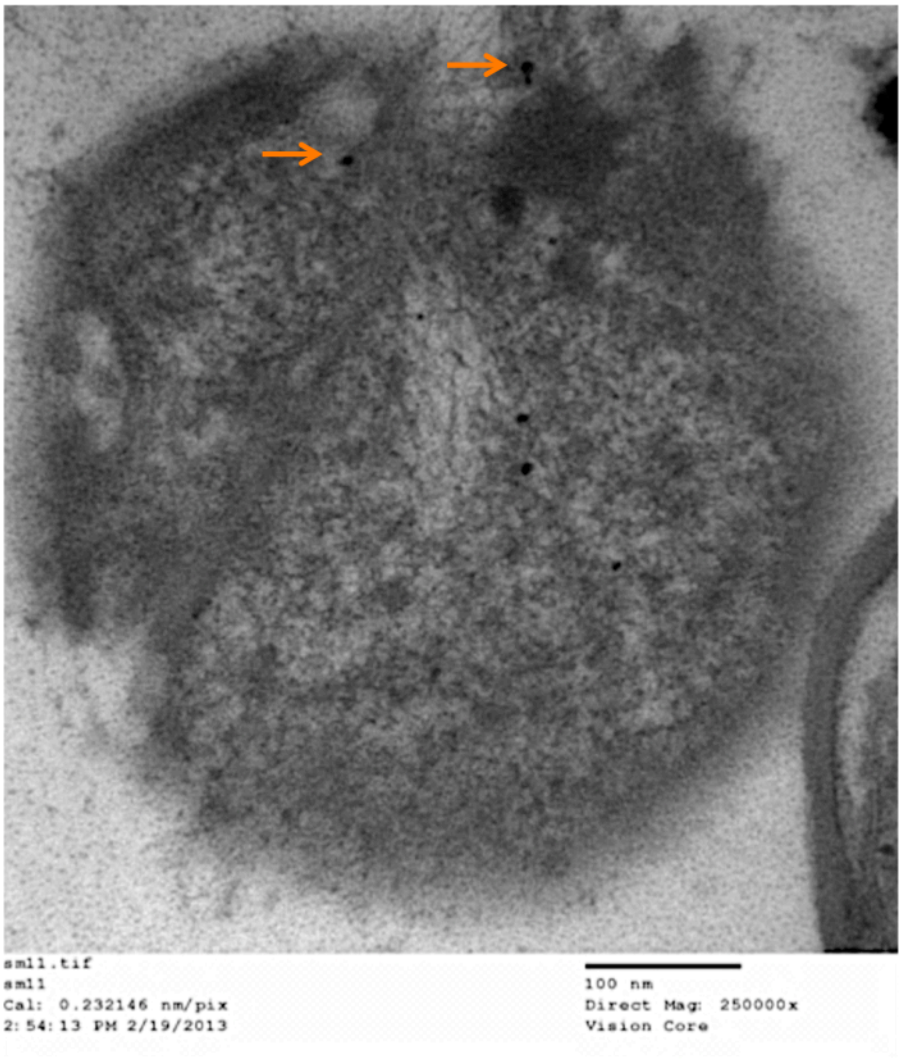

Figure 5.13: Conventional TEM images of partial rupture of *S. mutans* and leakage of bacterial organelles with particles included (arrow pointed)

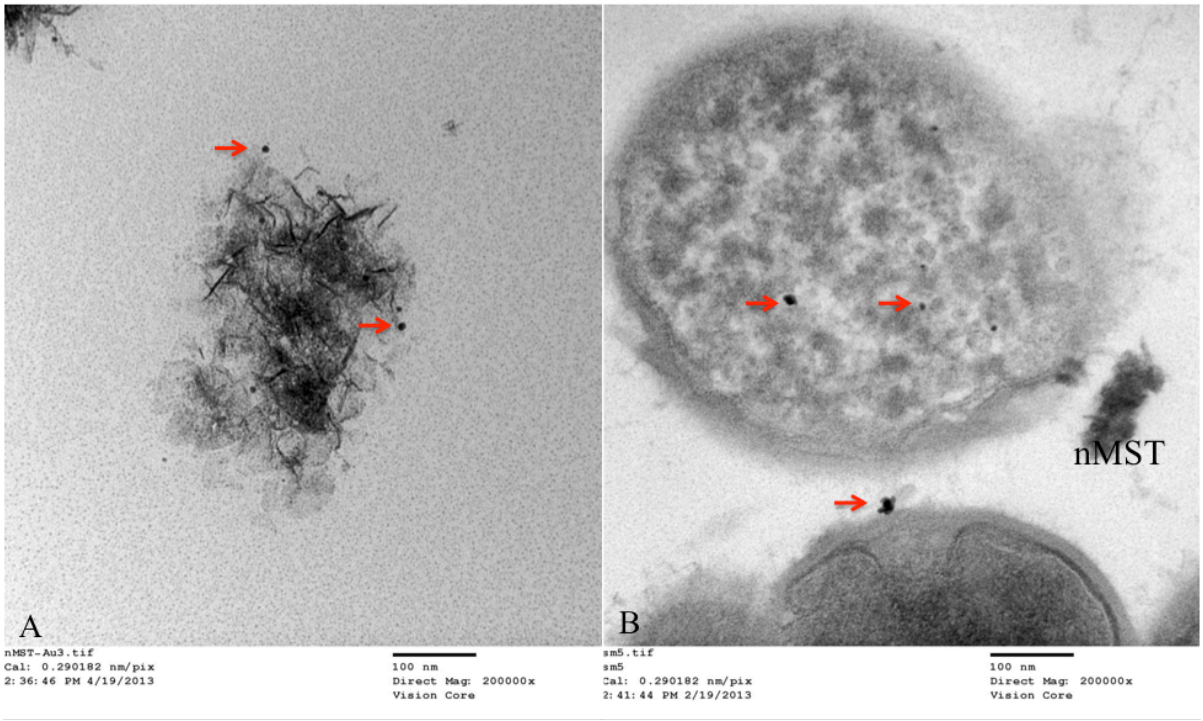

Figure 5.14: Transmission electron microscopy images of nMST-Au(III) suspension and *S. mutans* treated with nMST-Au(III).

(A) Arrows point gold (Au) nanoparticles in nMST compared in size, shape, and density with (B) Arrows point particles in *S. mutans* with nMST-Au(III). Image taken at magnification 250000X

DISCUSSION

After the L/D study in chapter 4, the effect of 400 mg/L nMST-Au(III) after 16 h exposure on bacterial integrity was examined using TEM analysis. According to conventional and tomographic TEM images of all bacteria, treated group had many more dead cells, compared to a few dead cells in untreated groups. nMST-Au(III) would have caused bacterial cell death. The TEM images show AuNPs were both attached to and internalized into bacterial cells. However, no nMST itself was closely attached or internalized into bacterial cells, which would support the notion that titanate itself has no antibacterial activity. The function of titanate as a carrier and gold ion-exchanger to target bacterial cells could improve antibacterial activity of AuNPs. Lokina *et al*. (2014) reported that synthesizing AuNPs with a reducing and stabilizing agent promoted the reduction of gold ions and form AuNPs, which resulted in a great antimicrobial activity against several organisms such as *Candida albicans* and *S. aureus*. The reducing and stabilizing agent promoted the reduction of gold ions and form AuNPs against bacterial cells. Zhao *et al*. (2010) studied antibacterial effect of AuNPs on Gram-Negative bacteria. Amino-substituted pyrimidine-capped AuNPs was tested with *P. aeruginosa* and *E. coli*. These pyrimidine-capped AuNPs were able to disrupt the bacterial cell membranes, leading to leakage of cytoplasmic components. The NPs were also internalized into bacterial cells, resulting in an interaction with bacterial DNA. Conversely, another study found AuNPs could only be absorbed onto *Salmonella typhimurium* cell wall but unable to penetrate into the bacterial cells. These AuNPs did not show a toxic effect on *S. typhimurium* (Wang *et al*., 2011). Antibacterial activity of AuNPs may require NPs interact or destroy intracellular structures. Corresponding to Zhao *et al.* (2010) TEM findings, AuNPs induced morphological changes of cell membrane and leakage of nucleic acids on *P. aeruginosa.* Interaction between AuNPs and

subcellular structures such as DNA and ribosome were determined. In 2012, Cui *et al.* reported that cell endocytosis of small AuNPs cause cytotoxicity of both human cervical carcinoma (HeLa) cells and *E. coli.* They also mentioned the relationship between the size of AuNPs and NPs toxicity. Small NPs could aggregate inside the cells leading to cell toxicity. In contrast, large NPs did not enter cells but attached onto cell surfaces, which may enhance cell growth.

According to these studies, two possible antibacterial activities of nMST-Au(III) mechanisms could be proposed. Once bacteria are exposed to nMST-Au(III), Au^{3+} ions could be released from nMST into the bacterial suspension and interact with bacteria by electrostatic attraction between negative charges of bacterial cell wall/membrane and positive charges of ions, and also enter the cells via ion transport. When Au^{3+} ions are internalized into the bacteria, they could be reduced to neutral gold atoms as observed in TEM images. Another explanation is that released Au^{3+} ions would be reduced to AuNPs outside the cells by bacteria themselves or surrounding environmental conditions. AuNPs are also able to attach to and be engulfed by bacteria as mentioned in previous studies (Zhao *et al*., 2010; Wang *et al*., 2011; Cui *et al*., 2012).

The tomographic TEM technique cannot detect AuNPs inside bacteria cells but only clusters of AuNPs attached to cell wall were shown obviously. This would be because a very small size of these particles, range from 1-20 nm, could not be detected by tomographic TEM technique. Microscopy may provide definitive representation of bacterial morphology but it is not quantitative.

In conclusion, conventional TEM imaging combined with tomographic technique confirmed that the nMST-Au(III) attached to bacterial cell wall and could be internalized into bacteria, leading to bacterial cell death.

CHAPTER 6

MOLECULAR OBSERVATION

INTRODUCTION

Recent evidence suggests that silver and gold nanoparticles would be able to reduce metabolic process of bacteria, since they suppress the expression of enzymes and proteins essential to ATP production, and alter bacterial membrane potential (Sondi and Salopek-Sondi, 2004; Yamanaka *et al*., 2005; Zhao *et al*., 2010). Cui *et al.* (2012) studied the molecular mechanisms of AuNPs' effects on *E. coli* and found that AuNPs affected the expression of many key genes. Their results showed that AuNPs significantly down-regulated bacterial gene expression related to ion transport, ATP metabolic process, proton transport, and purine ribonucleotide biosynthetic process. Conversely, genes relating to chemotaxis, flagellum assembly, response to chemical stimulus, and cellular component movement were up-regulated when bacteria were exposed to AuNPs. These results suggest that bacteria respond rapidly to AuNPs stimuli.

According to our TEM images, we found AuNPs attached to bacterial cell wall and internalized into cells, which suggests they may exert some physical interaction affecting bacterial membrane integrity. Molecular observation is also another aspect that would demonstrate how bacteria respond to gold-titanate. The objective for this aim was to quantify effects of gold-titanate on the expression of various *S. mutans* gene expression after treatment with three concentrations of nMST-Au(III) by using quantitative reverse transcription-

polymerase chain reaction (QRT-PCR). Twelve target genes were investigated as shown in Table 6.1 and *16s rRNA* was used to be a reference gene for normalization.

Our hypothesis was that gold-titanate NPs alter *S. mutans* mRNA expression when exposed to nMST-Au(III). These small-scale transcriptomics could let us better understand how bacteria react with NPs.

MATERIALS AND METHODS

Bacterial Strain and Gold-titanates

Following the protocol from chapter 2, *S. mutans* were grown aerobically as pure species in BHI at 37°C overnight. Low, medium, and high concentrations (10, 200, and 400 mg/L) of nMST-Au(III) were tested. Untreated bacteria were used as controls. *S. mutans* overnight cultures (10^8 CFUs/mL) were exposed to 400, 200, or 10 mg/L of nMST-Au(III) at time=0. All samples were cultured aerobically at 37°C and samples were collected from each culture at 6 h and 10 h.

Bacterial RNA Isolation and Complementary DNA (cDNA) Synthesis

After 6 h or 10 h incubation time, bacterial samples were centrifuged to remove cultured media and then washed once with PBS. Bacterial RNA were extracted by using TRIzol® Max™ Bacterial RNA Isolation Kit (Life technologies™, Grand Island, NY) and total RNA was purified by Ambion® TURBO DNA-free™ DNase Treatment and Removal Reagents (Life technologies™, Grand Island, NY) to remove contaminating DNA, according to manufacturer's protocol. Complementary DNA (cDNA) was prepared from 0.3 μg of total RNA using iScript™ cDNA Synthesis Kit (Bio-rad, Hercules, CA) by standard procedures.

Quantitative Reverse Transcription PCR (QRT-PCR)

The sequences of oligonucleotide primers used are listed in Table 6.1 **(**Ahn *et al*., 2005; Lévesque *et al*., 2005; Shemesh *et al*., 2007; Nascimento *et al.*, 2008; Kajfasz *et al.*, 2010; Wu *et al*., 2010; Xue *et al*., 2010; Stipp *et al*., 2013). QRT-PCR was conducted using an aliquot of total 15 ng cDNA with SYBR® Select Master Mix for CFX (Applied Biosystems®, Life technologies™, Grand Island, NY) and CFX96 Touch™ Real-Time PCR Detection System (Bio-Rad, Hercules, CA)**.** The reactions were set up in 96-well plates with a total volume of 20 µl containing 10 µl of 2X SYBR Green Select Mix, 1 µL of 0.3 µg cDNA, 1 µL of each 10 µM primer, and 7 µL RNase-free water. The amplification was run under the following conditions: 50 °C for 2 min, 95°C for 2 min, followed by 40 cycles of 95°C for 15 s and 59-64 °C (depending on primer sets for each gene) for 60 s. Melt-curve analysis was done at the end to verify that the detected signal was that of the expected amplification product and not possible primer-dimers. For each gene, QRT-PCR was performed in triplicate and normalized to the 16s rRNA reference gene. The relative fold changes in mRNA expression related to untreated group were analyzed by using the $2^{-\Delta\Delta Ct}$ Method (Livak and Schmittgen, 2001). All experiments were repeated three times independently.

Statistical Analysis

At each time point, the significant difference in mRNA gene expression at each concentration of nMST-Au(III) was compared to unstimulated control cells by using one-way analysis of variance (ANOVA) and Tukey's multiple comparisons test. In all experiments, the 95% confidence intervals and *p*-values indicate whether the difference is statistically significant.

Gene name	Forward Primer (5'-3')	Reverse Primer (5'-3')	Gene description and function
MsmE (SMU.878)	GTTTGCTTTAGCGGGAACAG	AATCGAATTTGGTTGGGAAAAG	Multiple sugar-binding ABC transporter/ sugar-binding protein
gtfB (SMU.1004)	AGCAATGCAGCCATCTACAAAT	ACGAACTTTGCCGTTATTGTCA	Glucosyltransferase-I/ glucans binding protein
atpA (SMU.1527)	GCACCCCTTGAAGTTCACGAG	GTTCACGCTCAGCCGAATCC	ATP synthase F_0F_1 subunit epsilon
dpr (SMU.540)	GAAGAAACAGTTGGCACATGGG	TTCCGTTTGAGCTGCTGTAAAG	Peroxidase resistance protein
rplS (SMU.1288)	CCGTACAGACATTCCTAACTTCC	ACACCAACACCGCTTGAAATC	50s Ribosomal Protein L19
ScrR (SMU.105)	TCGCATGGCATCCTTGAATCAG	TCAGCAGCTAATTGACCTCCAC	Transcriptional regulator; Repressor of sugar transport operon
grpE (SMU.81)	AGAGCGACAAAGTTTGCAGAGG	CAACAGCAAGAGCACGTTCAAG	Heat shock protein
LrgB (SMU.574)	GCCTTTGCCGTTCCACTTTAT	AACTGCTGATGATTTCCTTCCAA	Autolysin protein; Effector of murein hydrolase
*brpA (*SMU.410)	GGAGGAGCTGCATCAGGATTC	AACTCCAGCACATCCAGCAAG	Transcriptional regulator/ Biofilm formation/ cell envelope response
htrA2 (SMU. 2164)	AAGTTGTTAGACCCGCTCTTG	ACCGCTTGTGACATCACTTGG	Serine protease high temperature requirement A Controlling growth/ Protein repair

srtA (SMU. 1113)	GAAGCTTCCTGTAATTGGCG	TTCATCGTTCCAGCACCATA	Sortase A/ membrane-associated transpeptidase
ciaH (SMU.1128)	TTGGAAGAGGTCAGAAACATGAGA	CATCCCGACGGGCTAAATTA	Histidine kinase sensor: Two component signal transduction systems
16S rRNA	CGGCAAGCTAATCTCTGAAA	GCCCCTAAAAGGTTACCTCA	Reference gene

Table 6.1: Genes and oligonucleotide primer sequences for QRT-PCR used in this study

RESULTS

S. mutans gene expressions will likely be regulated in a different manner in response to various gold-titanate concentrations and exposure time. High and medium concentrations of nMST-Au(III) affected *S. mutans* gene expression whereas no significant difference in *S. mutans* gene expression between low concentration of nMST-Au(III) and control was observed. As shown in Figure 6.1, high and medium concentrations (200 and 400 mg/L) of gold-titanate NPs up-regulated *CiaH, dpr, htrA2* and *srtA* gene expression while no significant difference in relative fold change was observed for a group exposed to 10 mg/L when compared to control. All these genes were up-regulated at both 6 and 10 h.

At 6 h, the expression of *S. mutans gtfB* mRNA was increased in both 200 mg/L and 400 mg/L groups when compared to control (p-value <0.05 and <0.01, respectively). However at 10 h, only 200 mg/L group showed significant upregulation in *S. mutans gtfB* mRNA expression when compared to control (Figure 6.2)

According to Figure 6.3, at 6 h, the mRNA expression of *brpA* was up-regulated in 200 mg/L group (p-value <0.05), and at both 6 and 10 h this gene was dramatically down-regulated in 400mg/L (p-value <0.001) when compared to control. Similarly, at 6 and 10 h, *LrgB* was significantly down-regulated in 400 mg/L (p-value <0.05).

Relative fold changes of target genes, *atpA*, *grpE*, *MsmE*, *rplS*, and *ScrR*, compared to control, were presented in similar trend (Figure 6.4). At 6h, no significant difference of mRNA expression of these genes was observed among various concentrations of nMST-Au(III) and control. However, at 10 h, only 200 mg/L showed significant upregulation in these *S. mutans* genes when compared to control (p-value <0.01 or < 0.001, depending on each gene).

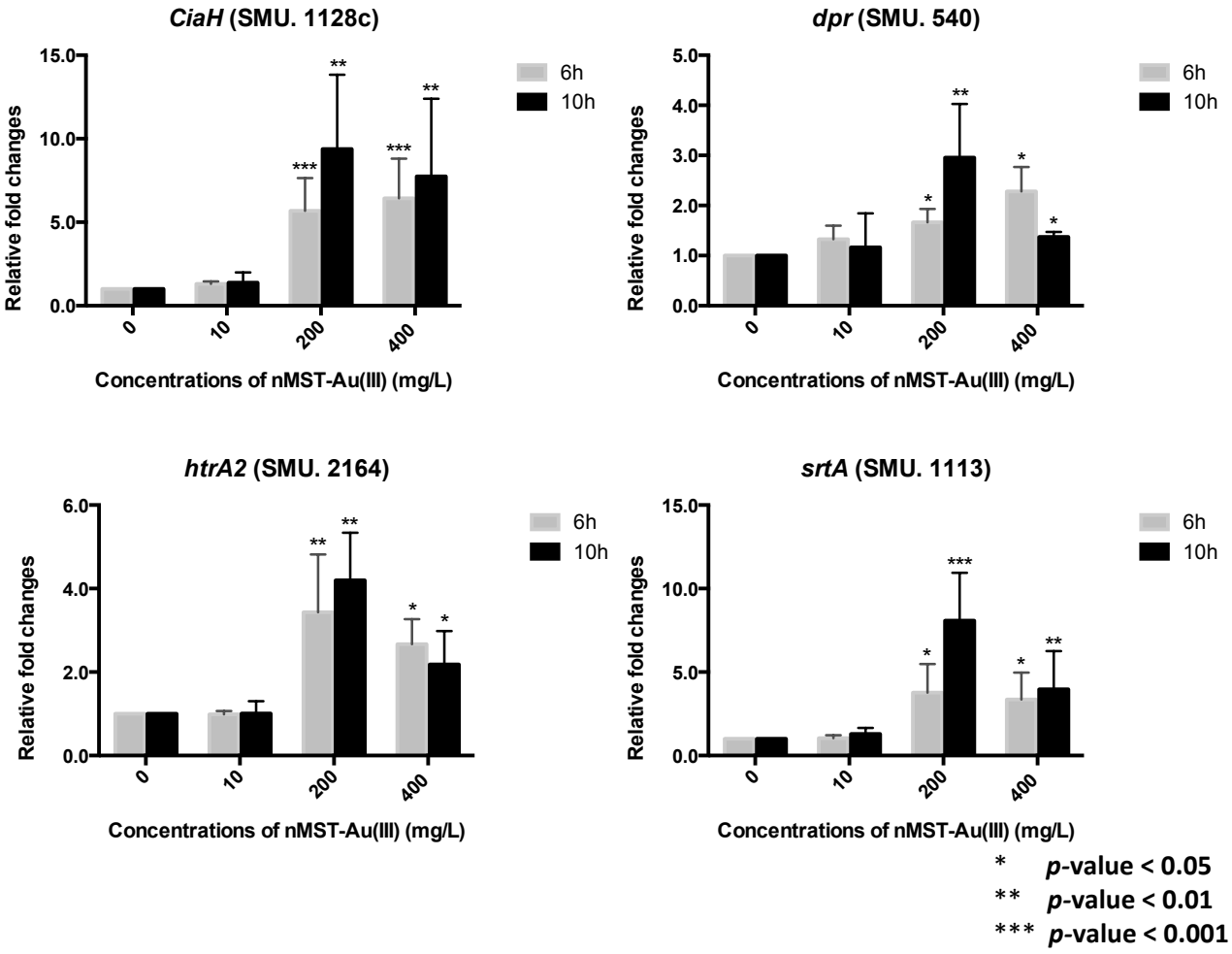

Figure 6.1: Relative fold changes of *CiaH, dpr, htrA2* and *srtA* gene expressions of *S. mutans* in response to 10, 200, or 400 mg/L nMST-Au(III) compared to untreated group (control) at 6 and 10 h. After incubation, mRNA expressions of these genes were determined by QRT-PCR. The mean ± SD values of mRNA expression of three independent experiments with each experiment set up in triplicate were expressed as relative fold change compared to untreated control bacterial culture.

*, p-value <0.05; **, p-value < 0.01; and ***, p-value < 0.001

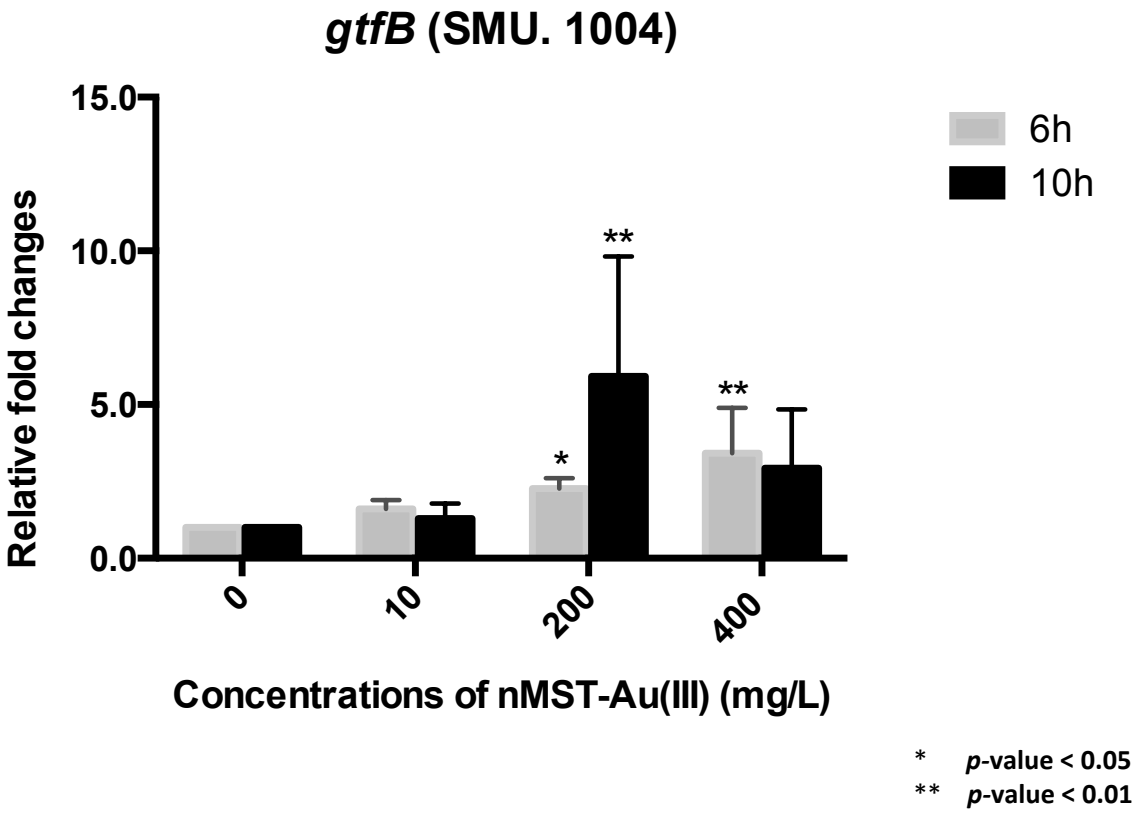

Figure 6.2: Relative fold changes of *gtfB* gene expressions of *S. mutans* in response to 10, 200, or 400 mg/L nMST-Au(III) compared to untreated group (control) at 6 and 10 h.

After incubation, mRNA expressions of these genes were determined by QRT-PCR. The mean ± SD values of mRNA expression of three independent experiments with each experiment set up in triplicate were expressed as relative fold change compared to untreated control bacterial culture.

*, p-value < 0.05; **, p-value < 0.01

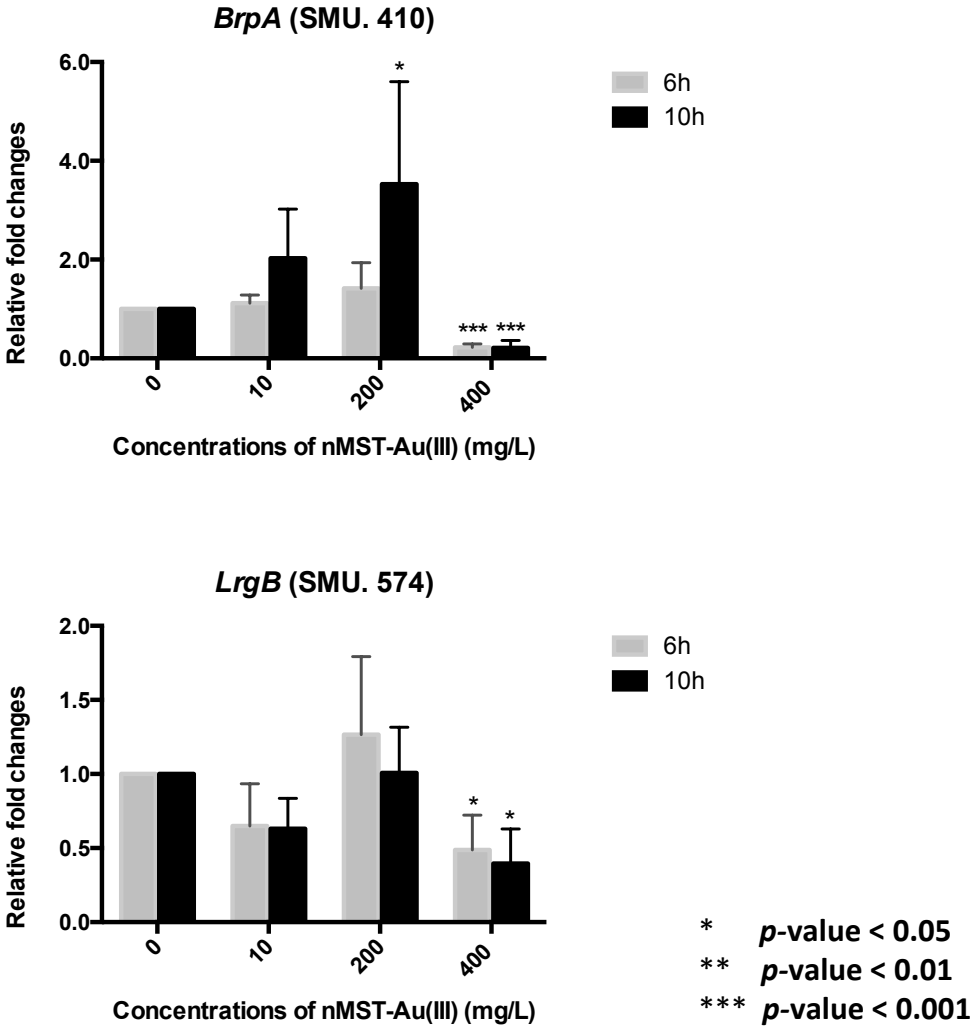

Figure 6.3: Relative fold changes of *brpA*, and *LrgB* gene expressions of *S. mutans* in response to 10, 200, or 400 mg/L nMST-Au(III) compared to untreated group (control) at 6 and 10 h. After incubation, mRNA expressions of these genes were determined by QRT-PCR. The mean ± SD values of mRNA expression of three independent experiments with each experiment set up in triplicate were expressed as relative fold change compared to untreated control bacterial culture. **, p-value < 0.01; ***, p-value < 0.001

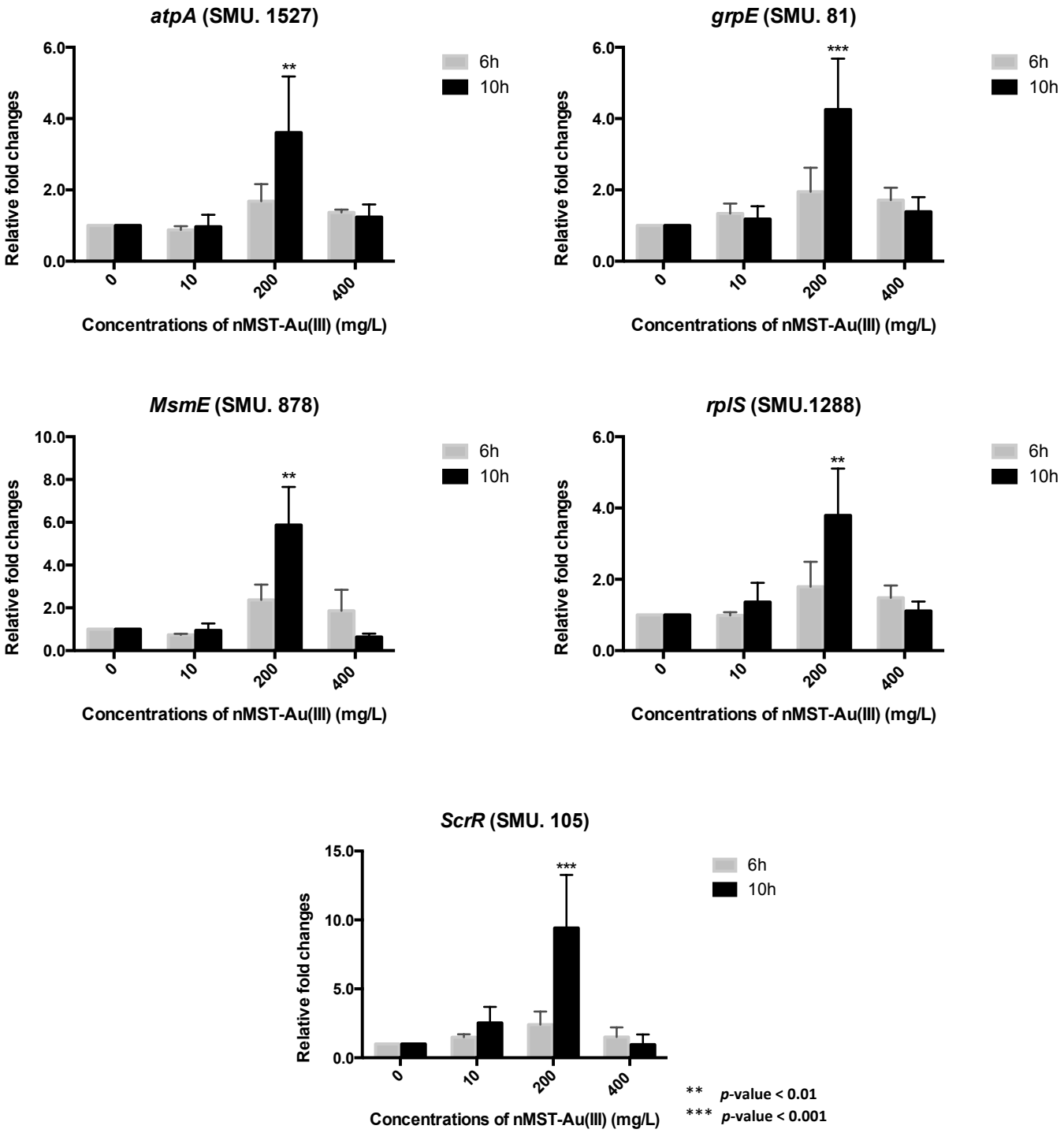
atpA (SMU. 1527)
grpE (SMU. 81)
MsmE (SMU. 878)
rplS (SMU.1288)
ScrR (SMU. 105)
Relative fold changes
Concentrations of nMST-Au(III) (mg/L)
6h
10h
0
10
200
400
**
***
** p-value < 0.01
*** p-value < 0.001

Figure 6.4: Relative fold changes of *atpA*, *grpE*, *MsmE*, *rplS*, and *ScrR* gene expressions of *S. mutans* in response to 10, 200, or 400 mg/L nMST-Au(III), when compared to untreated group (control) at 6 and 10 h. After incubation, mRNA expressions of these genes were determined by QRT-PCR. The mean ± SD values of mRNA expression of three independent experiments with each experiment set up in triplicate were expressed as relative fold change compared to untreated control bacterial culture.

**, p-value < 0.01; ***, p-value < 0.001

DISCUSSION

This study showed that *S. mutans* gene expression responded in various ways to each gold-titanate concentration and time. Some genes were regulated in similar trend as shown in Figure 6.1 and 6.4. Genes that are responsible for controlling growth/ protein repair (*htrA2*), peroxidase resistance protein (*dpr*), two components signal transduction systems (*CiaH*) were up-regulated by both high and medium concentrations. Corresponding to previous studies, these genes are associated with survival of *S. mutans* under stress conditions. *CiaH* and *htrA* were suggested to be genes involved in *S. mutans* acid stress response (Li *et al*., 2014). According to Cui *et al*. (2012) microarray study, *E. coli* mRNA gene expression related to chemotaxis and flagellum assembly were up-regulated when exposed to AuNPs. Chemotaxis is a bacterial mechanism that indicates efficient and rapidly respond to chemical stimuli. Transmembrane signal transducers from two signal transduction systems play a role to achieve this mechanism. Our results showed *CiaH* was up-regulated when exposed to 200 and 400 mg/L nMST-Au(III). This suggested that *S. mutans* responded to gold-titanate NPs quickly similar to *E. coli*. Correspondingly, *htrA2* main function is a key aspect of protein quality control. Its role in cellular physiology is to turn over damaged or malfolded proteins that accumulate, particularly under stress conditions such as heat, oxidative or acid stress. *HtrA2* is also regulated by the two component regulatory system (Biswas S and Biswas I, 2005; Kang *et al*., 2010). Furthermore, inducing oxidative stress results in essential protein and DNA damage. An iron-binding protein (*dpr*) is required for oxygen tolerance in *S. mutans.* This protein function does not directly react with oxygen and ROS. Possible protective role of this gene is to sequester iron (Fe) that can stimulate the generation of highly reactive and toxic oxygen species as hydroxyl radicals, which leads to protecting cells from peroxides and conferring oxygen tolerance (Yamamoto *et al*.,

2002; Yamamoto *et al*., 2004). Regarding our study, *dpr* may be up-regulated by aerobically cultured condition so investigating other antioxidant genes would be necessary to better understand whether nMST-Au(III) can induce oxidative stress leading to bacterial cell death.

SrtA (sortase A), a membrane-associated transpeptidase that covalently links a surface protein with a sorting signal to bacterial cell wall relating to pathologic virulence of *S. mutans* was up-regulated by both medium and high concentrations of nMST-Au(III). Deactivation of *SrtA* activity results in a potential reduction of *S. mutans* adhesion (Le´vesque *et al*., 2005; Huang et al., 2014). Other *S. mutans* virulence genes were also changed by medium concentration of nMST-Au(III). Glucosyltransferase I, *gtfB*, is necessary for production of glucan binding protein that is used for bacterial adhesion to tooth surfaces. At 6 h, *gtfB* was up-regulated in both medium and high concentrations but with longer exposure, no significant change in high concentration group was found. This suggests that proper exposure time and concentration of antibacterial agent are needed to attack bacteria. According to Bedran *et al*. (2014), sub-inhibitory concentration of broad-spectrum antibacterial agent, tricosan, promoted capacity of *S. mutans* biofilm formation and also increased *gtfB* mRNA expression. These results would verify that the effectiveness of therapeutic antibacterial agent is optimal when the concentration is above the minimum inhibitory concentration (MIC).

On the contrary, transcriptional regulator relating to biofilm formation and cell envelope response, *brpA*, was significantly up-regulated in medium concentration group but it was considerably down-regulated when exposed to high concentration of nMST-Au(III). *LrgB*, effector of murein hydrolase, working as selective removal of cell wall peptidoglycan and involving cell wall synthesis and cell division, also reacted to high concentration of nMST-Au(III) similar to *brpA*. These results suggest that high concentration might inhibit biofilm

formation and affect bacterial cell division. As previous studies have shown, biofilms help increase bacterial survival due to their functions enhancing poor antibiotic penetration, nutrient limitation, slow growth, adaptive stress responses, and formation of persister cells. Decreasing biofilm formation would enhance the ability of NPs against bacteria (Stewart, 2002). However, biofilm formation is influenced by many factors including bacterial communication. Investigation on quorum-sensing signaling system would help better comprehend this mechanism.

Surprisingly, genes playing roles in ATP synthase, ribosomal protein, repressor of sugar transport, ABC transporter and heat shock protein were slightly changed by nMST-Au(III). Upregulation of these genes after 10 h exposure of medium concentration was investigated but no significant change in gene expression was observed at the high concentration. This would suggest that medium concentration might not totally shut down bacterial metabolisms so bacteria would try to fight off by stimulating bacterial gene expression. The above finding is consistent with the study by Kohanski *et al*. (2010), in which authors demonstrated that using sublethal antibiotic dose stimulated bacterial response against drug and accelerated the formation of mutations leading to multidrug resistance.

Although our gene studies demonstrated that nMST-Au(III) has affected *S. mutans* mRNA expression, our data suggest that large-scale transcriptomic study would help us better understand how bacteria respond to gold-titanate NPs since bacteria require multiple gene expressions for biological function. Furthermore, proteomic study would also be an effective tool to investigate biological functions and support more evidences to explain how bacteria react to NPs.

In conclusion, gold-titanate NPs affected bacterial transcriptome in different ways depending on severity of stimuli and exposure time. Bacterial stress response genes may play an important role in bacterial survival. Inducing biofilm formation may be inhibited by gold-titanates NPs. These results confirmed that gold-titanate NPs would be a potential antibacterial agent against Gram-positive cariogenic bacteria.

CHAPTER 7

FUTURE STUDIES

According to our studies, we conclude that gold-titanates exert an antibacterial activity against Gram-positive cariogenic bacteria. Gold-titanate NPs, nMST-Au(III), showed the most effectiveness and could be a potential antimicrobial agent against these bacteria. This material affects both physical interaction and alteration of the bacterial transcriptome. TEM images show nMST-Au(III) particles attached to bacterial cell wall and were internalized into bacterial cells. Regarding QRT-PCR, nMST-Au(III) affected *S. mutans* mRNA expression in different manners with varied time and concentration. This work supports further development of gold-titanate NPs as a potential novel material to prevent dental caries**.** For clinical application, the incorporation of gold-titanate NPs into restorative, endodontic, or implant material is an exciting possibility. However, to design biomaterials for clinical use, further studies would provide strong evidences to support this material as antibacterial agent. Before clinical use, it is recommended that further experimental investigations should be undertaken in the following areas.

Transcriptomic study

Large-scale transcriptomics would help us examine entire changes of mRNA expression responding to external stimuli. Although, bacterial microarray may be an alternative tool to study the overall bacterial mRNA expression since it becomes a highly throughput and reasonably inexpensive method, hybridization-based approaches still have some limitations such as its complicated normalization methods and cross hybridization from high background levels. Currently, sequence-based approach, RNA-Seq, has become a more precise tool to investigate

mRNA expression. This method has been developed for transcriptomic profiling which can be used to analyze both eukaryotic and prokaryotic cells. As it directly determines the cDNA sequences, it does not require normalization of data (Wang *et al.,* 2009).

Proteomic study

Proteomics is the large-scale analysis of protein structures and function. After transcriptomics, proteomics is the next step in the study of biological systems, since changes in mRNA gene expression do not necessarily correlate to changes in functional protein levels. Proteomic study is an effective technique to help better understanding biological functions of cells and more information on proteomics would help us establish a greater degree of accuracy on this substance. (Pandey and Mann, 2000)

Biofilm study

In the oral cavity, microorganisms are likely to be in biofilms adhered to tooth surfaces. According to previous studies, compare to bacteria in planktonic culture, bacterial biofilms have dramatically higher resistance to antimicrobial agents including NPs and antibiotics (Allaker 2010; Pelgrift and Friedman, 2013). We suggest that antibacterial properties of gold-titanate NPs on biofilm growth should be further studied.

Biocompatibility study

Although some previous studies revealed that APT, MST, and nMST have minimal effect on mitochondrial activity of fibroblasts, monocytes, or human cell lines (Davis *et al*., 2007; Drury *et al*., 2014), cytotoxicity of gold-titanate NPs should be tested with several cell types, particularly oral tissue cells to prove that it has no significantly harmful effect on mammalian cells.

Clinical study

In the oral cavity, there are many factors that influence dental caries development. Saliva, pH, or oral biofilm formation are all able to change bacterial behaviors. Since our results showed only *in vitro* study of the antibacterial property of gold-titanates, clinical study of these NPs should be accomplished to help us understand more precisely what bacteria behaviors respond to NPs and bridge *in vitro* study to clinical treatment.

BIBLIOGRAPHY

Ajdić D, McShan WM, McLaughlin RE, Savić G, Chang J, Carson MB, *et al.* (2002). Genome sequence of *Streptococcus mutans* UA159, a cariogenic dental pathogen. *Proc Natl Acad Sci U S A* 99(22): 14434-9.

Ahn SJ, Lemos JA, Burne RA (2005). Role of *HtrA* in growth and competence of *Streptococcus mutans* UA159. *J Bacteriol* 187(9): 3028-38.

Ahn SJ, Wen ZT, Burne RA (2006). Multilevel control of competence development and stress tolerance in *Streptococcus mutans* UA159. *Infect Immun.* 74(3): 1631-42.

Allaker RP (2010). The use of nanoparticles to control oral biofilm formation. *J Dent Res* 89(11): 1175-1186.

Amarnath K, Kumar J, Reddy T, Mahesh V, Ayyappan SR, Nellore J (2012). Synthesis and characterization of chitosan and grape polyphenols stabilized palladium nanoparticles and their antibacterial activity. *Colloids and Surfaces B: Biointerfaces* 92: 254-261

Badet C, Thebaud NB (2008). Ecology of lactobacilli in the oral cavity: a review of literature. *Open Microbiol J* 2: 38-48.

Bedran TB, Grignon L, Spolidorio DP, Grenier D (2014). Subinhibitory concentrations of triclosan promote *Streptococcus mutans* biofilm formation and adherence to oral epithelial cells. *PLoS One* 9(2): e89059.

Bergmans L, Moisiadis P, Van Meerbeek B, Quirynen M, Lambrechts P (2005) Microscopic observation of bacteria: review highlighting the use of environmental SEM. *Int Endod J* 38(11): 775-88.

Biswas S, Biswas I (2005). Role of *HtrA* in surface protein expression and biofilm formation by *Streptococcus mutans*. *Infect Immun*. 73(10): 6923-34.

Boisselier E, Astruc D (2009). Gold nanoparticles in nanomedicine: preparations, imaging, diagnostics, therapies and toxicity. *Chemical Society Reviews* 38(6): 1759-1782.

Bowden GH, Hamilton IR (1998). Survival of oral bacteria. *Crit Rev Oral Biol Med.* 9(1): 54-85.

Bowman MC, Ballard TE, Ackerson CJ, Feldheim DL, Margolis DM, Melander C (2008). Inhibition of HIV fusion with multivalent gold nanoparticles. *Journal of the American Chemical Society* 130(22): 6896-6897.

Brown AN, Smith K, Samuels TA, Lu J, Obare SO, Scott ME (2012). Nanoparticles functionalized with ampicillin destroy multiple-antibiotic-resistant isolates of *Pseudomonas*

aeruginosa and *Enterobacter aerogenes* and methicillin-resistant *Staphylococcus aureus*. *Appl Environ Microbiol* 78(8):2768-74.

Burd A, Kwok CH, Hung SC, Chan HS, Gu H, Lam WK, Huang L (2007). A comparative study of the cytotoxicity of silver-based dressings in monolayer cell, tissue explant, and animal models. *Wound Repair Regen*. 15(1): 94-104.

Cho EC, Au L, Zhang Q, Xia Y (2010). The effects of size, shape, and surface functional group of gold nanostructures on their adsorption and internalization by cells. *Small* 6(4): 517-522.

Chung WO, Wataha JC, Hobbs DT, An J, Wong JJ, Park CH, *et al.* (2011). Peroxotitanate- and monosodium metal-titanate compounds as inhibitors of bacterial growth. *Journal of Biomedical Materials Research Part A* 97A (3): 348-354.

Cui Y, Zhao Y, Tian Y, Zhang W, Lu X, Jiang X (2012). The molecular mechanism of action of bactericidal gold nanoparticles on *Escherichia coli*. *Biomaterials* 33(7): 2327-2333.

Davis RR, Lockwood PE, Hobbs DT, Messer RL, Price RJ, Lewis JB, *et al*. (2007). In vitro biological effects of sodium titanate materials. *J Biomed Mater Res B Appl Biomater* 83(2): 505-11.

Davis RR, Hobbs DT, Khashaba R, Sehkar P, Seta FN, Messer RLW, *et al*. (2009). Titanate particles as agents to deliver gold compounds to fibroblasts and monocytes. *Journal of Biomedical Materials Research Part A* 93A (3): 864-869.

da Silva BR, de Freitas VA, Nascimento-Neto LG, Carneiro VA, Arruda FV, de Aguiar AS, *et al*. (2012). Antimicrobial peptide control of pathogenic microorganisms of the oral cavity: a review of the literature. *Peptides* 36(2): 315-21.

Drury JL, Jang Y, Taylor-Pashow KM, Elvington M, Hobbs DT, Wataha JC (2014). In vitro biological response of micro- and nano-sized monosodium titanates and titanate-metal compounds. *J Biomed Mater Res B Appl Biomater* [E-pub ahead of print May 13, 2014] In press.

Elvington MC, Tosten M, Taylor-Pashow KML, Hobbs DT (2012). synthesis and characterization of nanosize sodium titanates. *J Nanopart Res* 14:1114

García-Contreras R, Argueta-Figueroa L, Mejía-Rubalcava C, Jiménez-Martínez R, Cuevas-Guajardo S, Sánchez-Reyna PA, *et al.* (2011) Perspectives for the use of silver nanoparticles in dental practice. *Int Dent J*. 61(6): 297-301.

Gutierrez JA, Crowder T, Rinaldo-Matthis A, Ho MC, Almo SC, Schramm VL (2009). Transition state analogs of 5′-methylthioadenosine nucleosidase disrupt quorum sensing. *Nature Chemical Biology* 5(4): 251-257.

Hajipour MJ, Fromm KM, Ashkarran AA, Jimenez de Aberasturi D, de Larramendi IR, Rojo T, *et al*. (2012). Antibacterial properties of nanoparticles. *Trends Biotechnol*. 30(10): 499-511.

Hara AT, Zero DT (2010). The caries environment: saliva, pellicle, diet, and hard tissue ultrastructure. *Dent Clin North Am.* 54(3): 455-67.

Hasona A, Zuobi-Hasona K, Crowley PJ, Abranches J, Ruelf MA, Bleiweis AS, *et al.* (2006). Membrane composition changes and physiological adaptation by *Streptococcus mutans* signal recognition particle pathway mutants. *J Bacteriol* 189(4): 1219-30.

He S, Zhou P, Wang L, Xiong X, Zhang Y, Deng Y, *et al*. (2014). Antibiotic-decorated titanium with enhanced antibacterial activity through adhesive polydopamine for dental/bone implant. *J R Soc Interface*. 11(95): 20140169

Hobbs DT (2011). The properties and uses of sodium titanates and peroxotitanates. *Journal of the South Carolina Academy of Science* 9(1): 20-24.

Hobbs DT, Barnes MJ, Pulmano RL, Marshall KM, Edwards TB, Bronikowski MG, *et al*. (2005). Strontium and actinide separations from high level nuclear waste solutions using monosodium titanate 1. simulant testing. *Separation Science and Technology* 40(15): 3093-3111.

Huang P, Hu P, Zhou SY, Li Q, Chen WM (2014). Morin inhibits sortase A and subsequent biofilm formation in *Streptococcus mutans*. *Curr Microbiol*. 68(1): 47-52.

Hussain SM, Hess KL, Gearhart JM, Geiss KT, Schlager JJ (2005). In vitro toxicity of nanoparticles in BRL 3A rat liver cells. *Toxicol In Vitro* 19(7): 975-83.

Imazato S. (2009). Bio-active restorative materials with antibacterial effects: new dimension of innovation in restorative dentistry. *Dent Mater J*. 2009 28(1): 11-9.

Jayaseelan C, Rahuman AA, Kirthi AV, Marimuthu S, Santhoshkumar T, Bagavan A, *et al*. (2012). Novel microbial route to synthesize ZnO nanoparticles using *Aeromonas hydrophila* and their activity against pathogenic bacteria and fungi. *Spectrochimica Acta Part A: Molecular and Biomolecular Spectroscopy* 90: 78-84.

Jinnai H, Tsuchiya T, Motoki S, Kaneko T, Higuchi T, Takahara A (2012). Transmission electron microtomography in soft materials. *Microscopy (Oxf)* 62(2): 243-58.

Kajfasz JK, Rivera-Ramos I, Abranches J, Martinez AR, Rosalen PL, Derr AM, Quivey RG, Lemos JA (2010). Two *Spx* proteins modulate stress tolerance, survival, and virulence in *Streptococcus mutans. J Bacteriol* 192(10): 2546-56.

Kang KH, Lee JS, Yoo M, Jin I (2010). The influence of *HtrA* expression on the growth of *Streptococcus mutans* during acid stress. *Mol Cells*. 29(3): 297-304.

Kohanski MA, DePristo MA, Collins JJ (2010). Sublethal antibiotic treatment leads to multidrug resistance via radical-induced mutagenesis. *Mol Cell* 37(3): 311-20.

Kovvuru P, Mancilla PE, Shirode AB, Murray TM, Begley TJ, Reliene R (2014). Oral ingestion of silver nanoparticles induces genomic instability and DNA damage in multiple tissues. *Nanotoxicology*. [E‐pub ahead of print April 9, 2014] In press.

Lévesque CM, Voronejskaia E, Huang YC, Mair RW, Ellen RP, Cvitkovitch DG (2005). Involvement of sortase anchoring of cell wall proteins in biofilm formation by *Streptococcus mutans. Infect Immun* 73(6): 3773-7.

Li D, Shibata Y, Takeshita T, Yamashita Y (2014). A novel gene involved in the survival of *Streptococcus mutans* under stress conditions. *Appl Environ Microbiol*. 80(1): 97-103.

Li YH, Lau PC, Tang N, Svensäter G, Ellen RP, Cvitkovitch DG (2002). Novel two-component regulatory system involved in biofilm formation and acid resistance in *Streptococcus mutans*. *J Bacteriol*. 184(22): 6333-42.

Liu Y, Wang L, Zhou X, Hu S, Zhang S, Wu H (2011). Effect of the antimicrobial decapeptide KSL on the growth of oral pathogens and *Streptococcus mutans* biofilm. *Int J Antimicrob Agents* 37(1): 33-8.

Livak KJ, Schmittgen TD (2001). Analysis of relative gene expression data using real-time quantitative PCR and the $2^{-\Delta\Delta C}{}_{T}$ method. *Methods* 25(4): 402-8.

Lokina S, Suresh R, Giribabu K, Stephen A, Lakshmi Sundaram R, Narayanan V (2014). Spectroscopic investigations, antimicrobial, and cytotoxic activity of green synthesized gold nanoparticles. *Spectrochim Acta A Mol Biomol Spectrosc* 129C: 484-490.

Lopes I, Ribeiro R, Antunes E, Rocha-Santos TAP, Rasteiro MG, Soares AMVM, *et al*. (2012). Toxicity and genotoxicity of organic and inorganic nanoparticles to the bacteria *Vibrio fischeri* and *Salmonella typhimurium*. *Ecotoxicology* 21(3): 637-648.

Ma S, Izutani N, Imazato S, Chen JH, Kiba W, Yoshikawa R, *et al*. (2012). Assessment of bactericidal effects of quaternary ammonium-based antibacterial monomers in combination with colloidal platinum nanoparticles. *Dental Materials Journal* 31(1): 150-156.

Matsui R, Cvitkovitch D (2010). Acid tolerance mechanisms utilized by *Streptococcus mutans*. *Future Microbiology* 5(3): 403-417.

Mohanty S, Mishra S, Jena P, Jacob B, Sarkar B, Sonawane A (2012). An investigation on the antibacterial, cytotoxic, and antibiofilm efficacy of starch-stabilized silver nanoparticles. *Nanomedicine: Nanotechnology, Biology and Medicine* 8(6): 916-924.

Monteiro DR, Gorup LF, Takamiya AS, Ruvollo-Filho AC, Rodrigues de Camargo E, Barbosa DB (2009). The growing importance of materials that prevent microbial adhesion:

antimicrobial effect of medical devices containing silver. *International Journal of Antimicrobial Agents* 34(2): 103-110.

MubarakAli D, Arunkumar J, Nag KH, SheikSyedIshack KA, Baldev E, Pandiaraj D, *et al.* (2013). Gold nanoparticles from Pro and eukaryotic photosynthetic microorganisms—Comparative studies on synthesis and its application on biolabelling. *Colloids and Surfaces B: Biointerfaces* 103: 166-173.

Nascimento MM, Lemos JA, Abranches J, Lin VK, Burne RA (2008). Role of *RelA* of *Streptococcus mutans* in global control of gene expression. *J Bacteriol* 190(1):28-36.

Nyman M, Hobbs DT (2006). A family of peroxo-titanate materials tailored for optimal strontium and actinide sorption. *Chem. Mater*. 18: 6425–6435.

Pandey A, Mann M (2000). Proteomics to study genes and genomes. *Nature* 405 (6788): 837-46.

Pelgrift RY, Friedman AJ (2013). Nanotechnology as a therapeutic tool to combat microbial resistance. *Advanced Drug Delivery Reviews* 65:1803–1815.

Rai M, Yadav A, Gade A (2009). Silver nanoparticles as a new generation of antimicrobials. *Biotechnol Adv*. 27(1): 76-83.

Ramalingam K, Amaechi BT, Ralph HR, Lee VA (2012). Antimicrobial activity of nanoemulsion on cariogenic planktonic and biofilm organisms. *Archives of Oral Biology* 57(1): 15-22.

Roberts AP, Mullany P (2010). Oral biofilms: a reservoir of transferable, bacterial, antimicrobial resistance. *Expert Rev Anti Infect Ther* 8(12): 1441-50.

Roberts MC (1998). Antibiotic resistance in oral/respiratory bacteria. *Crit Rev Oral Biol Med* 9(4):522-540

Rosi NL, Giljohann DA, Thaxton CS, Lytton-Jean AKR, Han MS, Mirkin CA (2006). Oligonucleotide-modified gold nanoparticles for intracellular gene regulation. *Science* 312(5776): 1027-1030.

Sansone C, Van Houte J, Joshipura K, Kent R, Margolis HC (1993). The association of mutans streptococci and non-mutans streptococci capable of acidogenesis at a low pH with dental caries on enamel and root surfaces. *J Dent Res* 72:508-516.

Silvestry-Rodriguez N, Bright KR, Slack DC, Uhlmann DR, Gerba CP (2008). Silver as a residual disinfectant to prevent biofilm formation in water distribution systems. *Applied and Environmental Microbiology* 74(5): 1639-1641.

Shemesh M, Tam A, Steinberg D (2007). Expression of biofilm-associated genes of *Streptococcus mutans* in response to glucose and sucrose. *J Med Microbiol* 56 (Pt 11): 1528-35.

Sondi I, Salopek-Sondi B (2004). Silver nanoparticles as antimicrobial agent: a case study on *E. coli* as a model for Gram-negative bacteria. *Journal of Colloid and Interface Science* 275(1): 177-182.

Stewart PS (2002). Mechanisms of antibiotic resistance in bacterial biofilms. Int J *Med Microbiol* (2):107-13.

Stipp RN, Boisvert H, Smith DJ, Höfling JF, Duncan MJ, Mattos-Graner RO (2013). *CovR* and *VicRK* regulate cell surface biogenesis genes required for biofilm formation in *Streptococcus mutans*. *PLoS One* 8(3): e58271.

Sweeney LC, Dave J, Chambers PA, Heritage J (2004). Antibiotic resistance in general dental practice—a cause for concern? *Journal of Antimicrobial Chemotherapy* 53: 567–576

Su HL, Chou CC, Hung DJ, Lin SH, Pao IC, Lin JH, *et al.* (2009). The disruption of bacterial membrane integrity through ROS generation induced by nanohybrids of silver and clay. *Biomaterials* 30(30): 5979-5987.

Takahashi N, Nyvad B (2008). Caries ecology revisited: Microbial dynamics and the caries Process. *Caries Res* 42(6): 409-418.

Takahashi N, Nyvad B (2010). The role of bacteria in the caries process: Ecological Perspectives. *J Dent Res* 90(3): 294-303.

Tanzer JM, Livingston J, Thompson AM (2001). The microbiology of primary dental caries in humans. *J Dent Educ* 65(10): 1028-37.

Thomas M, Klibanov AM (2003). Conjugation to gold nanoparticles enhances polyethylenimine's transfer of plasmid DNA into mammalian cells. *Proceedings of the National Academy of Sciences* 100(16): 9138-9143.

Ul-Islam M, Shehzad A, Khan S, Khattak WA, Ullah MW, Park JK (2014). Antimicrobial and biocompatible properties of nanomaterials. *J Nanosci Nanotechnol* 14(1): 780-91.

Wang J, Gao J, Liu D, Han D, Wang Z (2012). Phenylboronic acid functionalized gold nanoparticles for highly sensitive detection of *Staphylococcus aureus*. *Nanoscale* 4(2): 451-454.

Wang S, Lawson R, Ray PC, Yu H (2011). Toxic effects of gold nanoparticles on *Salmonella typhimurium* bacteria. *Toxicology and Industrial Health* 27(6): 547-554.

Wang Z, Gerstein M, Snyder M (2009). RNA-Seq: a revolutionary tool for transcriptomics. *Nat Rev Genet.* 10(1): 57-63.

Wataha JC, Hobbs DT, Lockwood PE, Davis RR, Elvington MC, Lewis JB, *et al*. (2009). Peroxotitanates for biodelivery of metals. *Journal of Biomedical Materials Research Part B: Applied Biomaterials* 91B (2): 489-496.

Wataha JC, Hobbs DT, Wong JJ, Dogan S, Zhang H, Chung KH, *et al*. (2010). Titanates deliver metal ions to human monocytes. *J Mater Sci: Mater Med* 21(4): 1289-1295.

Wen ZT, Baker HV, Burne RA (2006). Influence of *BrpA* on critical virulence attributes of *Streptococcus mutans*. *J Bacteriol*. 188(8): 2983-92.

Whitman WB, Parte A, Goodfellow M, Kämpfer P, Busse HJ, Trujillo ME, *et al*. (2012). Bergey's Manual of Systematic Bacteriology / Vol. 5: The Actinobacteria. 2nd ed, New York: Springer.

Wu C, Ayala EA, Downey JS, Merritt J, Goodman SD, Qi F (2010). Regulation of *ciaXRH* operon expression and identification of the *CiaR* regulon in *Streptococcus mutans*. *J Bacteriol* 192(18): 4669-79.

Xiu ZM, Zhang QB, Puppala HL, Colvin VL, Alvarez PJJ (2012). Negligible particle-specific antibacterial activity of silver nanoparticles. *Nano Letters* 12(8): 4271-4275.

Xue X, Tomasch J, Sztajer H, Wagner-Döbler I (2010). The delta subunit of RNA polymerase, *RpoE*, is a global modulator of *Streptococcus mutans* environmental adaptation. *J Bacteriol* 192(19): 5081-92.

Yamamoto Y, Poole LB, Hantgan RR, Kamio Y (2002). An iron-binding protein, *Dpr*, from *Streptococcus mutans* prevents iron-dependent hydroxyl radical formation in vitro. *J Bacteriol*. 184(11): 2931-9.

Yamamoto Y, Fukui K, Koujin N, Ohya H, Kimura K, Kamio Y (2004). Regulation of the intracellular free iron pool by *Dpr* provides oxygen tolerance to *Streptococcus mutans*. *J Bacteriol.* 186(18): 5997-6002.

Yamanaka M, Hara K, Kudo J (2005). Bactericidal actions of a silver ion solution on *Escherichia coli*, studied by energy-filtering transmission electron microscopy and proteomic analysis. *Applied and Environmental Microbiology* 71(11): 7589-7593.

Zhao Y, Tian Y, Cui Y, Liu W, Ma W, Jiang X (2010). Small molecule-capped gold nanoparticles as potent antibacterial agents that target gram-negative bacteria. *Journal of the American Chemical Society* 132(35): 12349-12356.

Zhou Y, Kong Y, Kundu S, Cirillo JD, Liang H (2012). Antibacterial activities of gold and silver nanoparticles against *Escherichia coli* and *Bacillus Calmette-Guerin*. *Journal of Nanobiotechnology* 10(1): 19-27.

CURRICULUM VITAE

Trinuch Eiampongpaiboon, D.D.S., M.Sc.

EDUCATION

2001	Doctor of Dental Surgery (1st honors)
	Faculty of Dentistry, Mahidol University, Bangkok, Thailand
2005	Master of Science (Prosthodontics)
	Faculty of Dentistry, Mahidol University, Bangkok, Thailand
2007	Higher Graduate Diploma (Oral Rehabilitation)
	Faculty of Dentistry, Mahidol University, Bangkok, Thailand
2007	One year Master program in Implant Dentistry
	School of Dentistry, UCLA, Los Angeles, CA
2014	PhD (Oral Biology)
	School of Dentistry, University of Washington, Seattle, WA

POSITIONS AND HONORS

: Positions and Employments

2001	Head Director of Dental Department,
	Sankaburi Hospital, Chainat Province, Thailand
2004-present:	Lecturer
	Department of Prosthodontics, Faculty of Dentistry, Mahidol University,
	Bangkok, Thailand

: Other Experiences and Professional Memberships

2000-2001	Scientific Committee of Mahidol Dental Student Society
2001-Present	Member, Thai Dental Council
2001-Present	Member, The Dental Association of Thailand
2003-Present	Member, Thai Prosthodontic Association
2003-Present	Member, Thai Operative Dentistry Society
2004-2008	Student Advisory Board, School of Dentistry, Mahidol University, Bangkok, Thailand
2005	Scientific subcommittee of The 4th Biennial Congress of Asian Academy of Prosthodontics in conjunction with The 6th Annual Scientific Meeting of Thai Prosthodontic Association
2006, 2007	Visiting researcher, School of Dentistry, University of Florida, Gainesville, USA

: Honors and Achievements

2001	Dental Student 1st Award in Prosthodontics, Department of Prosthodontics Mahidol University, Bangkok, Thailand
2001	First Class Honors in Doctor of Dental Surgery
2004	Supported in part by the Thesis Grant, Faculty of Graduate studies, Mahidol University, Bangkok, Thailand
2009-Present	Royal Thai Scholarship